Photosynthetic conversion of CO_2 to hyaluronic acid by engineered strains of the cyanobacteri~~a~~um *Synechococcus* sp. PCC 7002

Lifang Zhang [a], Tiago Toscano Selão [a], Peter J. Nixon [a, b] and Birgitta Norling [a]

[a] School of Biological Sciences, Nanyang Technological University, Singapore

[b]Sir Ernst Chain Building-Wolfson Laboratories, Department of Life Sciences, Imperial College London, S. Kensington Campus, London, SW7 2AZ, UK

Corresponding author: Birgitta Norling, School of Biological Sciences, Nanyang Technological University, Singapore**;** email: ibnorling@ntu.edu.sg

Abstract

Hyaluronic acid (HA), consisting of alternating N-acetylglucosamine and glucuronic acid units, is a natural polymer with diverse cosmetic and medical applications. Currently, HA is produced by overexpressing HA synthases from gram-negative *Pasteurella multocida* (encoded by *pmHAS*) or gram-positive *Streptococcus equisimilis* (encoded by *seHasA*) in various heterotrophic microbial production platforms. Here we introduced these two different types of HA synthase into the fast-growing cyanobacterium *Synechococcus* sp. PCC 7002 (Syn7002) to explore the capacity for producing HA in a photosynthetic system. Our results show that both HA synthases enable Syn7002 to produce HA photoautotrophically, but that overexpression of the soluble HA synthase (PmHAS) is less deleterious to cell growth and results in higher production. Genetic disruption of the competing cellulose biosynthetic pathway increased the HA titer by over 5-fold (from 14 mg/L to 80 mg/L) and the relative proportion of HA with molecular mass greater than 2 MDa. Introduction of *glmS* and *glmU*, coding for enzymes involved in the biosynthesis of the precursor UDP-N-acetylglucosamine, in combination with partial glycogen depletion, allowed photosynthetic production of 112 mg/L of HA in 5 days, an 8-fold increase in comparison to the initial PmHAS expressing strain. Addition of *tuaD* and *gtaB* (coding for genes involved in UDP-glucuronic acid biosynthesis) also improved the HA yield, albeit to a lesser extent. Overall our results have shown that cyanobacteria hold promise for the sustainable production of pharmaceutically important polysaccharides from sunlight and CO_2.

Keywords

Cyanobacteria; metabolic engineering; hyaluronic acid; photoautotrophic production

Abbreviations

WT – wild type

GFP – Green Fluorescent Protein

RBS – ribosome binding site

UDP– uridine diphosphate

IPTG– Isopropyl β-D-1-thiogalactopyranoside

PEG– polyethylene glycol

1. Introduction

Cyanobacteria are gaining attention as hosts for photosynthetic production of high-value molecules due to their easier genetic manipulation in comparison to other photosynthetic systems and favourable growth rates [1, 2]. Metabolic engineering of cyanobacteria has successfully led to the production of a wide range of industrially relevant products [3, 4]. However, apart from a very recent report on the production of heparosan [5], the use of cyanobacteria to produce pharmaceutically important polysaccharides remains relatively unexplored.

Hyaluronic acid (HA) is a unique biopolymer composed of alternating β-1,3-N-acetyl glucosamine and β-1,4-glucuronic acid disaccharide units [6]. Its distinctive moisturizing and viscoelastic properties, coupled to a lack of immunogenicity and toxicity, have led to a wide range of proven and marketed applications for HA within the cosmetic and biomedical industries [7]. The global HA market was valued at USD 7.2 billion in 2016 and is expected to reach USD 15.4 billion by 2025 [8], with. However, mmost of the commercial HA is currently being either isolated from animal sources, such as rooster combs, or made by microbial fermentation [9]., While production by modified group C *Streptococcus* strains under specific growth conditions can reach 6-7 g/L in fed-batch fermentation [10, 11], it has several drawbacks, such as with the potential problem of contamination by endotoxins. The increased demand for HA and arising safety concerns have led researchers to use synthetic biology and metabolic engineering approaches to develop alternative sources of HA production.

Two types of HA synthase, catalyzing the final HA synthesis step, are commonly used in metabolic engineering efforts, most commonly the enzymes PmHAS from *Pasteurella multocida* and SeHasA (or SzHasA) from *Streptococcus* species. Successful HA production was previously demonstrated in genetically modified non-pathogenic *Bacillus subtilis* and *Escherichia coli* strains overexpressing different HA synthases, along with the relevant

precursor synthesis enzymes [12-17]. Although HA titers in these modified strains are promising, with some being used in industrial scale processes [16], their production is completely based on fermentative processes, requiring the input of substantial amounts of carbon feedstocks, such as glucose or sucrose. On the other hand, photosynthetic bio-manufacturing processes for the sustainable and economic production of value-added chemicals are an increasingly promising solution to these issues. Cyanobacteria can naturally converts CO_2 into diverse carbohydrates and have high intracellular nucleotide sugar pool sizes [18]. Additionally, some strains have already been engineered to produce and excrete either soluble sugars (such as sucrose [19]) or polysaccharides, e.g. crystalline cellulose [20] or heparosan [5].

Synechococcus sp. are one of the major groups of marine cyanobacteria and its representatives play an important role in the global food chain and carbon cycle [21]. While these strains are also known to produce lipopolysaccharides (LPS), the immune response to different *Synechococcus* sp. LPS is either negative [22] or at least 3 orders of magnitude below that of other gram-negative bacteria [23], and they are therefore considered as safe hosts for biotechnological applications [24]. In this study, we aimed to engineer *Synechococcus* sp. PCC 7002 (hereafter Syn7002), a fast growing and robust chassis strain, into a photosynthetic HA production system, thus demonstrating that cyanobacteria have the potential to become viable and safe alternatives for the sustainable production of biomedically relevant polysaccharides.

2. Material and Methods

2.1. Strains and culture conditions

Wild-type *Synechococcus* sp. PCC 7002 (a kind gift from Donald Bryant, Pennsylvania State University, USA) and all derivative strains were grown in medium AD7 [25] and supplemented with antibiotics as required, namely chloramphenicol (10 µg/mL) and/or

kanamycin (100 µg/mL). Liquid cultures and plates were grown in an atmosphere of CO_2-enriched (1% (v/v)) air, under continuous illumination (300 µmol photons m^{-2} s^{-1}) at 38 °C, as previously described [25]. Growth was monitored by measuring OD_{730} in a plate reader (Hidex Sense, Hidex) and utilizing an in-house generated 70-point calibration curve (R^2=0.9818) converting OD_{730} in the plate reader to that measured using a 1 cm light path table top spectrophotometer (Cary 300Bio, Varian), using AD7 as blank. Dry cell weight at 5 days was measured as previously described [25]. All growth measurements were performed using biological triplicates (n=3). To test HA production, cultures were pre-adjusted to an OD_{730}=1, induced by addition of 1 mM IPTG, and samples collected at the time points indicated. Cell pellets and supernatants were stored at -20 °C until further use.

2.2. Cyanobacterial strain construction

Genes encoding two HA synthases, *pmHAS* and *seHasA,* (the latter with a C-terminal FLAG tag), as well as *B. subtilis* genes encoding UDP-glucose dehydrogenase (*tuaD*), UDP-glucose pyrophosphorylase (*gtaB*), and the *E. coli* genes encoding glutamine amidotransferase (*glmS*) and acetyl-CoA acetyltransferase/pyrophosphorylase (*glmU*, a homologue of *gcaD* in *B. subtilis*) were codon-optimized for Syn7002 and synthesized by GenScript (Hong Kong). The expression of both HA synthase genes was controlled by an IPTG inducible promotor, $P_{cLac143}$, based on plasmid *pAcsA*-$P_{cLac143}$-*YFP* (a kind gift from Brian Pfleger, University of Wisconsin-Madison, USA) [26]. The *tuaD* and *gtaB* genes were synthesized as an artificial operon, under control of the strong constitutive P_{cpc560} promoter [27], with a second artificial operon containing *glmS* and *glmU*, controlled by the strong constitutive P_{cpt} promoter [28]. In all cases, the strong AGGAGA RBS sequence was utilized, with a random 8 bp DNA sequence between RBS and the initial ATG codon [28]. All enzymes utilized were purchased from NEB unless otherwise specified and all primers used are listed in Table S1. DNA fragments were PCR amplified with Q5 DNA polymerase, purified using the EZ-10 Spin Column PCR Products

Purification Kit (Bio-Basic, Canada) and assembled either using the pEASY-Uni Seamless Cloning and Assembly Kit (TransGen Biotech, China), following manufacturer's instructions, or by *E. coli* mediated assembly [29]. Supercompetent *E. coli* cells (Stellar, TaKaRa) were used for all cloning steps and were grown in LB medium supplemented with antibiotics as required - ampicillin (100 µg/mL), chloramphenicol (25 µg/mL) or kanamycin (50 µg/mL). The sequence of all constructed plasmids (Table ~~S1~~S2) was confirmed by Sanger sequencing. Syn7002 transformation was performed according to standard protocols [30]. Full genomic segregation in modified strains was confirmed by colony PCR using specific primers. A list of all strains generated in this work is presented in Table 1.

2.3. Fluorescence microscopy and western blot

Preparation of Syn7002 cells for confocal microscopy was performed as described earlier [31]. Essentially, cells from IPTG-induced cultures were collected and blotted on a 1% agarose gel pad (prepared with AD7 medium) for image analysis. Laser scanning confocal microscopy was performed using an LSM710 (Carl Zeiss), with a 1.4 NA Plan-Apo 60x oil immersion lens used as an objective at a zoom factor of 10 and excitation at 488 nm. Image analysis was carried out using the Zen software (Carl Zeiss, version 2.3). Cell size estimates were made using the measuring tool in the Zen software and calculating averages and standard deviations from 15-20 cells from each strain, imaged at the same magnification.

Whole-cell lysates were isolated as previously described and subjected to western blot analysis [32]. 10 µg total proteins were separated on 12% precast SDS-PAGE gels (BioRad), transferred onto PVDF membranes and probed with primary antibodies raised in rabbit against a synthetic PmHAS peptide (NDNDLKSMNVKGAS, amino acids 860 to 874, prepared by GenScript, Hong Kong) and/or a monoclonal mouse anti-FLAG M2 antibody (F3165, Sigma-Aldrich).

2.4. Cyanobacterial HA preparation and quantification by ELISA

HA production by engineered Syn7002 strains was routinely assessed by measuring the HA released into the growth medium at the indicated time points. Cells were collected by centrifugation (3000 g, 10 min, room temperature) and the cleared supernatant was used to assay~~for~~ HA levels~~assay~~. To concentrate HA from cyanobacterial cultures, 3 volumes of ice-cold ethanol were added to the cleared supernatants and the resulting pellets wereas dried in air and re-suspended in deionised H_2O for further use [33]. To evaluate the HA secretion ability of different strains, released HA (R-HA), capsular HA (bound to the cell surface, CPS-HA) and intracellular HA (intra-HA) were isolated according to previously described methods [12, 34], with whole cell lysates for intra-HA quantification prepared according to Selão et al [32]. HA quantification was performed using a Hyaluronan Quantikine ELISA Kit (DHYAL0, R&D systems, USA), following the manufacturer's instructions, either directly or by diluting samples with AD7 prior to quantification, and absorbance of the ELISA strips was measured using the Hidex Sense plate reader.

2.5. Characterization of HA by HPLC, LC-MS/MS and FTIR

Cyanobacterial HA was further analysed using an UFLC Prominence (Shimadzu, Japan) equipped with a size-exclusion chromatography column (Shodex OHpak, SB806 M HQ, 8.0 mm×300 mm, 13µm particle size, Shimadzu), coupled to a UV detector (Shimadzu, Japan) and a differential refractive index detector (dRI, Optilab rEX, Wyatt Technology, USA). The mobile phase was a 0.1 M NaCl solution and all chromatography runs were performed at 0.5 mL/min. Samples were filtered through 0.2 µm Whatman Puradisc 13 syringe filters (GE Healthcare, USA) prior to injection and 150 µL were used in each run. Chromatography data was recorded and analyzed by the ASTRA software (version 5.3, Wyatt Technology, USA). All peaks detected by the dRI detector were collected and saved at -20 °C until further use. The molecular mass of detected peaks was estimated by comparison to the elution times of PEG

analytical standard (ReadyCal Set, #02393, Sigma-Aldrich) and of commercial HA with known molecular mass (2-2.2 MDa, #51967, Sigma-Aldrich).

LC-MS/MS was used to characterize the forming units of HA polymer produced by the PmHAS-expressing strains following hyaluronidase digestion. HPLC-purified sample was precipitated using ethanol as described above, and subjected to hyaluronidase (#H3506, Sigma-Aldrich) digestion according to manufacturer's instructions. After confirmation of complete digestion using both the HA ELISA assay and HPLC, the resulting fragments were analyzed by LC-MS/MS, using a Xevo-TQ-S (Waters, Milford, USA) mass spectrometry system, coupled to an ACQUITY UPLC system (Waters) with a 2.1mm x 100mm HSS T3 Column, 1.8µm particle size (Waters), as previously described [35]. Cyanobacterial HA from HPLC eluted peaks was also subjected to Fourier transform infrared spectroscopy (FTIR) analysis after precipitation with cold ethanol. 10 µL samples were evenly spotted on a horizontal ZnSe ATR element (Pike Technologies) and dried under a stream of dry, CO_2-free air. The respective spectra (average from 200 scans at 4 cm^{-1} resolution) were recorded between 4000-650 cm^{-1} using an FTIR Nicolet Nexus 470 instrument (Thermo Scientific), purged with dry, CO_2-free air and equipped with an MCT/A detector cooled with liquid nitrogen.

3. Results and Discussion

3.1. Overexpression of HA synthase in Syn7002

As with all cyanobacteria sequenced so far, Syn7002 lacks homologues of the known HA synthases and is not known to naturally produce HA. However, an analysis of its predicted metabolic network (using the KEGG database) suggests that this organism has all the enzymes required to synthesize the two HA precursor molecules, UDP-GlcUA and UDP-GlcNAc (Fig. 1). Both of these UDP-sugars, as well as their precursors, are used for cyanobacterial cell wall

biosynthesis and could theoretically be redirected to the biosynthesis of HA or similar polysaccharides [5].

We used a previously described IPTG-inducible expression system (the $P_{cLac143}$ promoter system [28]) to regulate the expression of PmHAS or SeHasA, and integrated the two respective genes at the *acsA* locus of Syn7002 (Fig. 2A). Fully segregated strains (HA01 harboring *pmHAS* and HA03 containing *seHasA*), as well as C-terminal GFP-tagged versions (HA02 and HA04 respectively), were confirmed by colony PCR (Fig. 2B). Immunoblotting experiments confirmed that expression of both HA synthases was induced upon IPTG addition (Fig. 2C), with overexpression of PmHAS and SeHasA resulting in the appearance of either a 110 kDa or a 49 kDa protein, respectively. Overexpression of either HA synthase impacted cell growth, with SeHasA having a more severe effect (Fig. S1A).

HA synthase activity in these strains was evaluated by quantifying HA present in the medium after IPTG induction using a specific ELISA Kit, which uses a specific HA-binding protein for recognition and quantification of HA with molecular mass higher than 35 kDa [37]. While WT cultures produced no detectable HA, strains expressing either of the HA synthases produced moderate amounts of HA upon induction. For strain HA01, the HA concentration in the medium increased from 9.8±0.85 mg/L (at 5 days post-induction) to 31.9±4.0 mg/L (at 10 days post-induction) while strain HA03 had an overall lower HA production in comparison to the HA01 strain (Fig. 2D). However, as the higher HA concentration at 10 days was linked to a decline in the cell density of the culture, all subsequent HA production experiments were performed with cell cultures at an earlier growth phase (up to 5 days post-induction).

To understand better the reasons behind the low productivity of strain HA03 (expressing the integral membrane SeHasA synthase), the location of both enzymes was studied by adding a C-terminal superfolder-GFP (sfGFP) tag. This tag did not negatively affect HA synthesis activity, with similar amounts of HA detected in the growth medium 5 days post-IPTG

induction (Fig. S1B). Confocal microscopy revealed that cells expressing sfGFP-tagged derivatives of PmHAS (HA02) and SeHasA (HA04) were larger than WT, with SeHasA expression having a more pronounced effect (Fig. S2). While overexpressing sfGFP alone in Syn7002 resulted in cells with average dimensions of 1.9±0.1 µm×1.3±0.1 µm (length × width), accumulation of PmHAS-sfGFP in strain HA02 lead to a slight increase in cell size (2.7±0.7 µm×1.7±0.1 µm) and accumulation of SeHasA-sfGFP in strain HA04 significantly increased cellular dimensions (4.1±0.9 µm×2.3±0.2 µm). sfGFP fluorescence was concentrated in the cytoplasm of HA02 cells but mostly found in random patches in HA04. Thylakoid membranes in HA04 cells also seemed distorted, possibly by mistargeting of integral membrane protein SeHasA or due to accumulation of HA in the lumenal space. Consequently, all further engineered strains used PmHAS, ~~as~~ since this soluble HA synthase was more benign and more productive than its integral counterpart.

3.2. Characterization of HA produced by PmHAS in Syn7002

In addition to the specific ELISA assay, we employed several alternative methods to positively identify the polymers produced upon expressing PmHAS. Strain HA01 was used to isolate released cyanobacterial polysaccharides by ethanol precipitation from culture supernatants 5 days after IPTG induction. The obtained material (HA01-HA) was analyzed by hyaluronidase digestion, HPLC-SEC, and LC-MS/MS. Hyaluronidase digestion of HA01- HA, similarly to that of commercial HA, resulted in a loss of detection by the ELISA assay and a shift to much smaller polymer sizes, as detected by HPLC-SEC (Fig. S3). LC-MS/MS analysis of the hyaluronidase-digested samples identified the typical HA disaccharide~~s~~ with m/z 395.7 and tetrasaccharide with m/z 774.9 both in the digested HA01-HA sample and the commercial HA control (Fig. S4), further verifying the identity of the produced polymer.

3.3. Cellulose removal benefits HA production

The biosynthesis of HA in our modified Syn7002 strains relies solely on intermediates derived from photosynthetic carbon fixation (see Fig. 1), which are also commonly used by cells for the generation of internal glycogen storage granules [38] or are converted to UDP-Glucose (UDP-Glc) for synthesis of cell wall components, such as cellulose or other types of polysaccharides [39]. The carbon flux towards HA synthesis is therefore potentially limited by these other pathways. As the biosynthesis pathways involved in cell wall polysaccharides have not been fully characterized in Syn7002, we focused on the possible effect of blocking cellulose synthesis or lowering the glycogen level on HA production. Therefore, several deletion mutants were constructed to investigate their influence on HA production (Fig. 3A).

Deletion of either of the two glycogen synthase genes (*glgA1* and *glgA2*) had only minor effects on HA production in comparison to the HA01 strain (Fig. S5), even though each deletion should increase glucose-1-phosphate pools and decrease glycogen biosynthesis by ≈50% [40]. The limited effects of partial glycogen depletion on HA production may imply that either Glc-1-P could not be efficiently converted to UDP-GlcUA or the limiting step for HA production might be related to the synthesis of the other precursor, UDP-GlcNAc. Cellulose, an insoluble polysaccharide that is also produced by some cyanobacteria, is synthesized in Syn7002 by a cellulose synthase (CesA), the deletion of which was shown to be essential for high-level cellulose production in engineered Syn7002 [20]. Our results show that overexpression of PmHAS in strain HA08 (a *cesA* knock-out background) led to a mild growth impairment in comparison to both WT and the basic HA01 strain, which was offset by substantially improved HA production, reaching 80.4±4.2 mg/L on the 5th day post-induction (in comparison to 14.8±2.0mg/L in HA01, Fig. 4A). This marked improvement in HA production upon disruption of cellulose synthesis may be due to a higher flux from UDP-glucose to UDP-GlcUA, one of the HA precursors, as mentioned above. On the other hand, as cellulose was found to form a laminar layer in Syn7002, located in the vicinity of the

peptidoglycan layer [20], there is also the possibility that endogenous cellulose removal may facilitate excretion of HA by removal of a physical barrier.

3.4. HA yield is improved by overexpression of enzymes involved in precursor biosynthesis

A commonly utilized strategy in other bacterial strains engineered for HA production is to strengthen the biosynthesis of the precursors UDP-GlcUA and/or UDP-GlcNAc [41]. Studies using recombinant strains of *B. subtilis* overexpressing either SeHasA or PmHAS have shown that UDP-glucuronic acid (UDP-GlcUA) biosynthesis can be a limiting step for production of HA [14, 16], with co-overexpression of PmHAS and TuaD-GtaB allowing a maximum titer of 6.8 g/L. Conversely, the co-overexpression of PmHAS with GcaD (a homologue of GlmU), involved in synthesis of UDP-GlcNAc, produced very low molecular mass HA and improved HA titer to a lesser extent (2.4 g/L) [14]. A similar strategy also allowed modified *E. coli* strains to reach a final titer of 3.8 g/L in a fed-batch reactor [13]. Although most of the enzymes involved in HA precursor biosynthesis have predicted homologs in cyanobacteria (as shown in Fig. 1), the expression, functionality and regulation of those Syn7002 gene products have so far not been studied and it was therefore preferable to manipulate precursor biosynthesis by expressing heterologous enzymes.

An artificial operon to improve UDP-GlcNAc biosynthesis, P_{cpt}-*glmS*-*glmU*, was introduced into either the *glpK* neutral locus in strain HA11 [26] or the *glgA1* site in strain HA12 (Fig. 3). HA production increased in both strains, to 111.9±10.6 mg/L in HA12 and 35.9±5.5 mg/L in HA11 (Fig. 4A), demonstrating that enhanced biosynthesis of UDP-GlcNAc improves HA yields in Syn7002, an effect magnified when glycogen synthesis was simultaneously inhibited. Although HA production was not improved by merely deleting *glgA1* (or *glgA2*), the combination of lower glycogen biosynthesis with increasing synthesis of the precursor UDP-GlcNAc did successfully divert carbon flow to the final product, HA.

Separately, to increase UDP-GlcUA precursor pools, the P_{cpc560}-*tuaD-gtaB* operon was introduced into the other glycogen synthase locus (*glgA2*) of Syn7002 in strain HA13 (Fig. 3). HA production (29.3±9.5 mg/L) improved in comparison to HA01, albeit to a lesser extent than in strain HA12 (Fig. 4A). Interestingly, overexpression of UDP-GlcUA-related enzymes in Syn7002 did not influence HA titers as strongly as in heterotrophic organisms [14, 16, 17]. As heterologous HA production diverts intermediates away from cell wall biogenesis, growth was affected by HA production, with higher HA titers generally resulting in lesser growth (lower OD_{730}), particularly in the case of strain HA12, which had both the lowest cell density and the highest titer (Fig. 4A).

3.5. Released HA is only a minor fraction of the total production

As the mechanism for HA secretion in PmHAS-utilizing bacterial strains is unknown, we tested the excretion efficiency of producing strains by quantifying HA isolated from different locations. We found that in all the strains tested large amounts of HA were retained within the cells, ranging from 42% to roughly 88%. Strain HA12, with the UDP-GlcNAc pathway enhanced, was able to release a higher portion of HA into the medium, however the vast majority of the product (about 60%) was still trapped within the cell (Fig. 4B). Interestingly, strain HA08 with cellulose removed had the highest amount of capsular HA among all the strains. Nearly 50% of the total HA production for strain HA08 was found attached to the cell surface (Fig. 4B). One possible explanation is that removal of the cellulose layer facilitates secretion of HA, even if it is not completely released from the cell surface. In light of these results, it seems clear that, even though all the generated strains improved their HA production capabilities, secretion and release of such large polymer is still a major bottleneck. Clearly, the mechanism responsible for polysaccharide (HA) excretion in cyanobacteria is unable to efficiently export the large amount of HA produced by the engineered strains, which may also be one of the causes for the growth defects observed.

Total HA production of these strains was calculated by summing up the values obtained from different fractions and photosynthetic CO_2 partitioning was estimated according to measured dry cell biomass, the carbon fraction in HA of 44.4% and assuming that total cellular carbon ias 51.3% of cell biomass (as previously described [42]). Strain HA12 has the highest carbon partitioning efficiency (≈25%), a substantial increase in comparison to strain HA01 (converting <2% of fixed carbon to HA). Overexpression of GlmS and GlmU most likely diverts carbon flow from the primary photosynthetic intermediate fructose-6-phosphate, to synthesize UDP-GlcNAc, resulting in comparatively better carbon partitioning (Fig. 4B and Table S3), though at the expense of cell growth (Fig. 4A). Strain HA08 (with *cesA* deleted) showed a similar CO_2 partitioning to HA as strain HA13 (roughly 16%), but with a better growth performance, which may be more suitable for sustainable production of HA.

3.6. The molecular weight of excreted HA varies with different pathway modifications

Size-exclusion chromatography was used to characterize the molecular mass of the excreted polymers produced by the different strains, using 2-2.2 MDa commercial HA and 1 MDa PEG polymers as standards-. All samples from the different strains had two major peaks, one with a molecular mass greater than 2-2.2 MDa and a smaller one with mass greater than 1 MDa, referred to as "UHMW-HA" and "HMW-HA" respectively (Fig. 5). These peaks were further analyzed by HA quantification (Fig. 5B) and FTIR (Fig. S6). The quantification of the HA content of each eluted peak generally fits with the peak intensity shown by the chromatography spectra, indicating that the introduced modifications, while possibly influencing precursor levels, resulted in changes to the size of produced HA. As shown in Fig. 5, strains HA08 and HA12 had a higher proportion of the UHMW-HA, whereas strains HA01 and HA13 strains excreted mainly HMW-HA. The reason for this is unclear but might be related to the different regulation mechanisms at the level of polymerization and secretion, as previously seen in engineered *B. subtilis* strains [14]. FTIR spectra for the major chromatography peaks isolated

from the HA-producing strains, but not from WT Syn7002, were very similar to that of commercial HA (Fig. S6), again confirming the identity of the produced polymers.

4. Conclusions

This work shows that cyanobacteria are promising hosts to produce biomedically-relevant sugar polymers solely by photosynthesis, paving the way for the sustainable production of hyaluronic acid. Heparosan was recently shown to be produced by heterologous expression of a heparosan synthase in *Synechococcus* sp. PCC 7942, although with an extremely low yield (3 µg/L) [5]. The best performing strain in the current report (HA12) shows a several thousand-fold improvement in comparison to the heparosan-producing strains, perhaps owing to codon-optimization of the introduced enzymes, more robust growth of our cyanobacterial host in comparison to *Synechococcus* sp. PCC7942 and iterative metabolic engineering. HA production was successfully improved by using different strategies, such as deleting the endogenous cellulose synthase gene and overexpressing precursor biosynthesis enzymes and, especially in the case of the UDP-GlcNAc pathway, combining precursor biosynthesis with glycogen depletion was particularly beneficial for production, though at the cost of growth performance.

Even if these results are encouraging, several issues still remain to be solved before cyanobacteria can compete with the yields observed in heterotrophic hosts. Increasing the photosynthetic performance of cyanobacteria is a commonly used strategy for improved yield, as this could improve up-stream precursor pools for HA synthesis and other metabolites [43]. PmHAS-mediated HA secretion may be further improved by down-regulating other competing pathways (such as O-antigen or peptidoglycan synthesis), which might also remove physical barriers further improving HA excretion.

As environmentally -conscious processes become increasingly relevant in relation to the mitigation of climate changes, the development of efficient engineered cyanobacterial cell

factories could allow biopolymer production without competing for food-grade materials, arable land or freshwater resources, thus contributing to a more sustainable bio-economy.

Acknowledgements

This work was supported by NTU grants M4080306 to BN and M4081714 to PJN. The authors would like to thank Dr. Wahyu Surya (SBS, NTU) for assistance with the size-exclusion chromatography analysis of samples and Associate Professor Jaume Torres (SBS, NTU) for access to his FTIR spectrometer. We would also like to thank the NTU Optical Microscopy for cell imaging analysis and NTU Phenomics Centre for LC-MS/MS analysis of HA fragments. The authors are grateful to Prof. Bertil Andersson for his constant support and encouragement and his pivotal role in establishing the CyanoSynBio@NTU laboratory.

Contributions

LZ, TTS, PJN and BN conceptualized and designed the present study. TTS performed the initial cloning of HA synthases in the expression vector, LZ performed all other strain engineering, cyanobacteria cultivation, production tests and product analysis. All authors contributed to data analysis, manuscript drafting and revision, agree to authorship and approve the final manuscript for submission.

Conflict of interest

Declarations of interest: none.

Tables and Figures

Table 1. Engineered cyanobacterial strains used for HA production in the study.

Strain name	Genotype	Characteristics
HA01(HA02)	Δ*AcsA*::$P_{cLac143}$-*pmHAS(-sfGFP)*	HA producing, without or with sfGFP
HA03(HA04)	Δ*AcsA*::$P_{cLac143}$-*seHasA(-sfGFP)*	HA producing, without or with sfGFP
HA06	Δ*glgA2*::Km^R +Δ*AcsA*::$P_{cLac143}$-*pmHAS*	Partial glycogen depletion, HA producing
HA07	Δ*glgA1*::Cm^R +Δ*AcsA*::$P_{cLac143}$-*pmHAS*	Partial glycogen depletion, HA producing
HA08	Δ*cesA*::Cm^R +Δ*AcsA*::$P_{cLac143}$-*pmHAS*	Cellulose depletion, HA producing
HA11	Δ*glpK*::P_{cpt}-*glmS-glmU*-Cm^R +Δ*AcsA*::$P_{cLac143}$-*pmHAS*	Overexpression of heterologous UDP-GlcNAc pathway enzymes, HA producing
HA12	Δ*glgA1*::P_{cpt}-*glmS-glmU*-Cm^R +Δ*AcsA*::$P_{cLac143}$-*pmHAS*	Overexpression of heterologous UDP-GlcNAc pathway enzymes, partial glycogen depletion, HA producing
HA13	Δ*glgA2*::P_{cpc560}-*tuaD-gtaB*-Km^R +Δ*AcsA*::$P_{cLac143}$-*pmHAS*	Overexpression of heterologous UDP-GlcUA pathway enzymes, partial glycogen depletion, HA producing

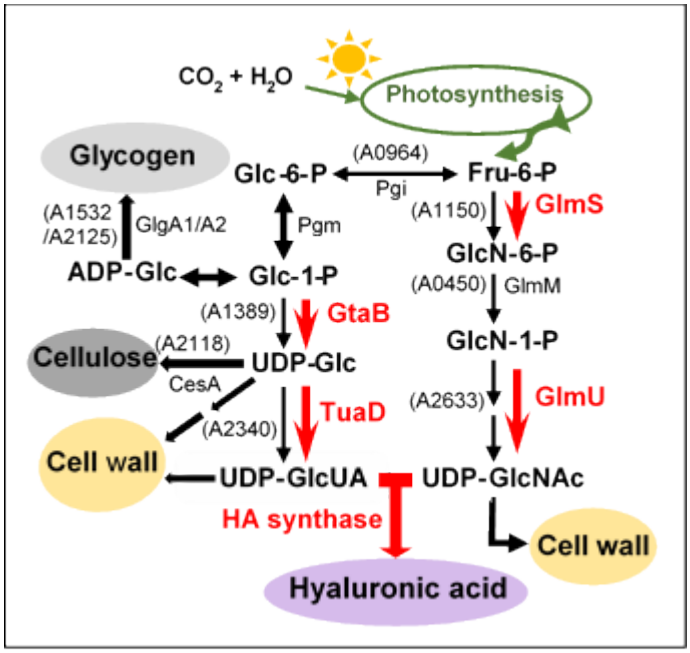

Figure 1. Schematic pathway for hyaluronic acid precursor biosynthesis in Syn7002 (adapted from [16]). Red arrows indicate heterologous enzymes commonly used to strengthen the precursors biosynthesis and HA formation in heterotrophic bacteria; - equivalent, functionally proven or predicted enzymes from Syn7002 are shown in brackets. Selected potential competing pathway, such as glycogen, cellulose or cell wall biosynthesis are also marked with coloured-in circles. Glc-6-P: glucose-6-phosphate; Glc-1-P: glucose-1-phosphate; ADP-Glc: ADP-glucose; UDP-Glc: UDP-glucose; UDP-GlcUA: UDP-glucuronic acid; Fru-6-P: fructose-6-phosphate; GlcN-6-P: glucosamine-6-phosphate; GlcN-1-P: glucosamine-1-phosphate; GlcNAc-1-P: N-acetylglucosamine-1-phosphate; UDP-GlcNAc: UDP-N-acetylglucosamine; TuaD: UDP-glucose dehydrogenase; GtaB: UDP-glucose pyrophosphorylase; GlmS: glutamine amidotransferase; GlmU: acetyl-CoA acetyltransferase/pyrophosphorylase; GlgA1/A2: glycogen synthase A1/A2; CesA: cellulose synthase; Pgi: phosphoglucoseisomerase; Pgm: phosphoglucomutase

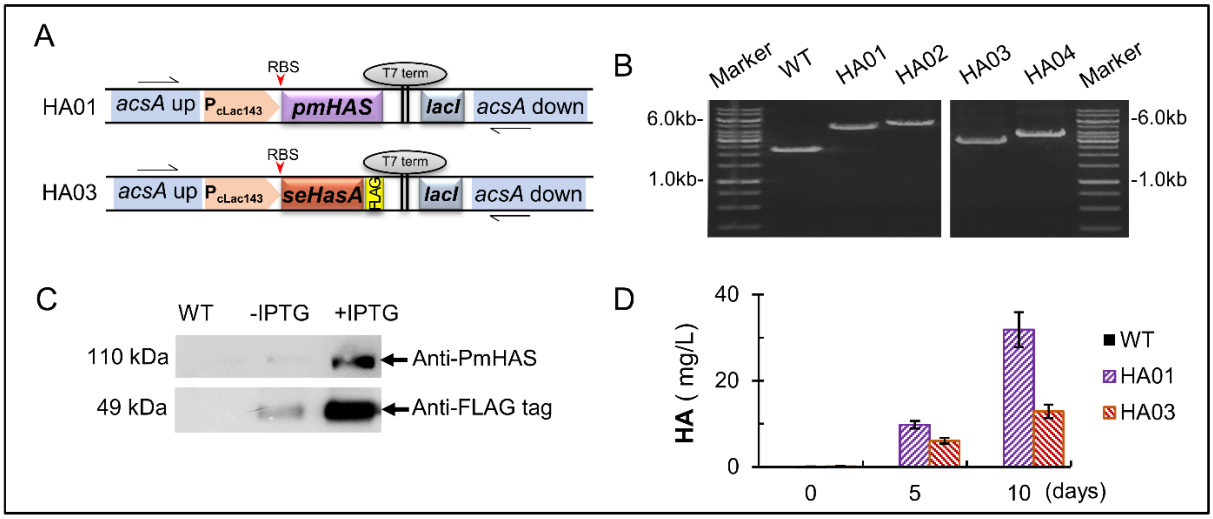

Figure 2. Introduction of two different HA synthases into Syn7002. **A.** Artificial operons used for expression of different HA synthases from the *acsA* locus of Syn7002, controlled by the inducible promoter $P_{cLac143}$. **B.** Genomic DNA PCR analysis of strains with *pmHAS* (HA01) or *seHasA* (HA03), as well as their *sfGFP*-tagged version (HA02 and HA04), with specific primers listed in Table S1. Expected PCR sizes are 4773 bp for strain HA01, 5508 bp for strain HA02, 3279 bp for HA03, 3983 bp for HA04 and 2303 bp for the *acsA* WT locus. **C.** Western blot analysis of PmHAS or SeHasA expression in response to IPTG addition, using either anti-PmHAS or anti-FLAG antibodies, respectively. **D.** Quantification of HA in the growth medium in cultures induced with 1mM IPTG, at the time points indicated. Error bars represent standard deviation of three biological replicates (n=3), measured in duplicate. HA01: Δ*acsA*::$P_{cLac143}$-*pmHAS*; HA02: Δ*acsA*::$P_{cLac143}$-*pmHAS-sfGFP*; HA03: Δ*acsA*::$P_{cLac143}$-*seHasA*; HA04: Δ*acsA*::$P_{cLac143}$-*seHasA-sfGFP*.

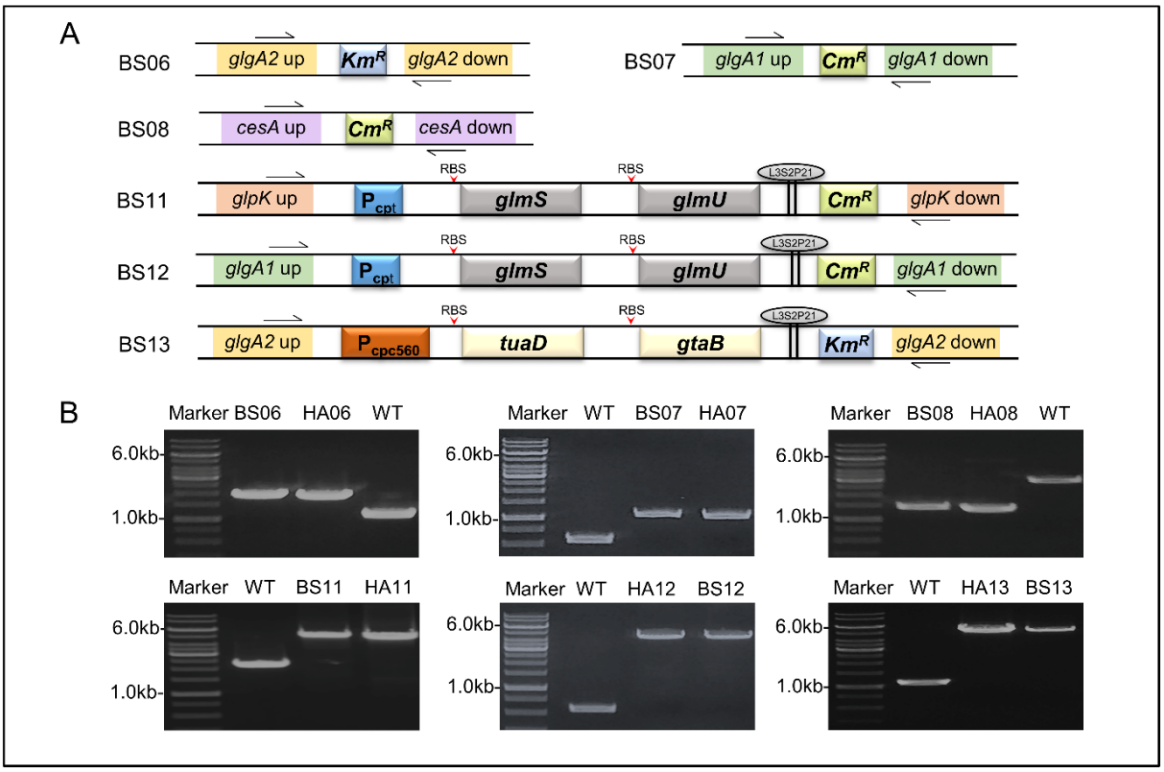

Figure 3. Overview of the different modifications for improved PmHAS-dependent HA production in Syn7002. **A.** Schematic images of constructs used for deletion of competing pathways and heterologous expression of precursor biosynthesis artificial operons. **B.** Gel images of gDNA PCR segregation tests for all background strains (BS##) and their corresponding PmHAS containing strains (HA##) constructed in this work. Primers used for segregation testing are listed in Table S1. Expected PCR product sizes are: 1470bp (BS06 and HA06), 1108bp (BS07 and HA07), 1365bp (BS08 and HA08), 4723bp (BS11 and HA11), 4955bp (BS12 and HA12) and 4199bp (BS13 and HA13). The corresponding expected PCR sizes in WT are 576bp (*glgA1*), 938bp (*glgA2*), 2097bp (*glpK*) and 2863bp (*cesA*). HA06: Δ*glgA2*::*Km*^{R} +Δ*acsA*::P$_{cLac143}$-*pmHAS*; HA07: Δ*glgA1*::*Cm*^{R} +Δ*acsA*::P$_{cLac143}$-*pmHAS*; HA08: Δ*cesA*::*Cm*^{R} +Δ*acsA*::P$_{cLac143}$-*pmHAS*; HA11: *glpK*::P$_{cpt}$-*glmS-glmU-Cm*^{R}+Δ*acsA*::P$_{cLac143}$-*pmHAS*; HA12: Δ*glgA1*::P$_{cpt}$-*glmS-glmU-Cm*^{R}+Δ*acsA*::P$_{cLac143}$-*pmHAS*; HA13: Δ*glgA2*::P$_{cpc560}$-*tuaD-gtaB-Km*^{R}+Δ*acsA*::P$_{cLac143}$-*pmHAS*

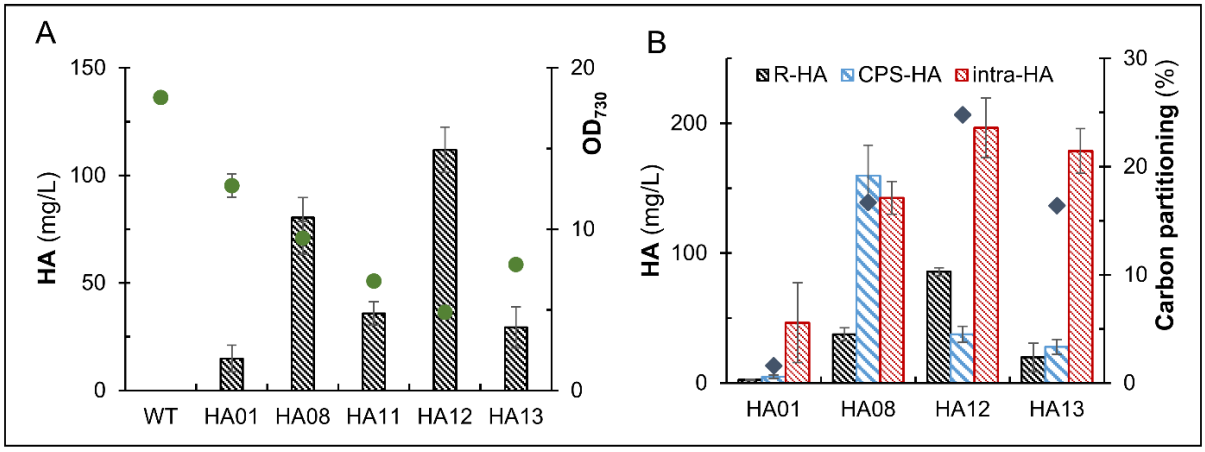

Figure 4. HA production by different strains. **A.** HA production (bar graphs) and cell density (dot plots) comparison at 5 days post IPTG induction. **B.** Assessment of HA ~~excretion by HA~~ quantification in different fractions, as well as the calculated photosynthethic carbon partitioning to total HA production (diamond plots). R-HA: HA released into growth medium; CPS-HA: capsular HA attached to cell surface; intra-HA: intracellular HA. Error bars represent standard deviation of technical triplicates. HA01: Δ*acsA*::$P_{cLac143}$-*pmHAS*; HA08: Δ*cesA*::*Cm*^{R} +Δ*acsA*::$P_{cLac143}$-*pmHAS*; HA11: *glpK*::P_{cpt}-*glmS-glmU-Cm*^{R}+Δ*acsA*::$P_{cLac143}$-*pmHAS*; HA12: Δ*glgA1*::P_{cpt}-*glmS-glmU-Cm*^{R}+Δ*acsA*::$P_{cLac143}$-*pmHAS*; HA13: Δ*glgA2*::P_{cpc560}-*tuaD-gtaB-Km*^{R}+Δ*acsA*::$P_{cLac143}$-*pmHAS*.

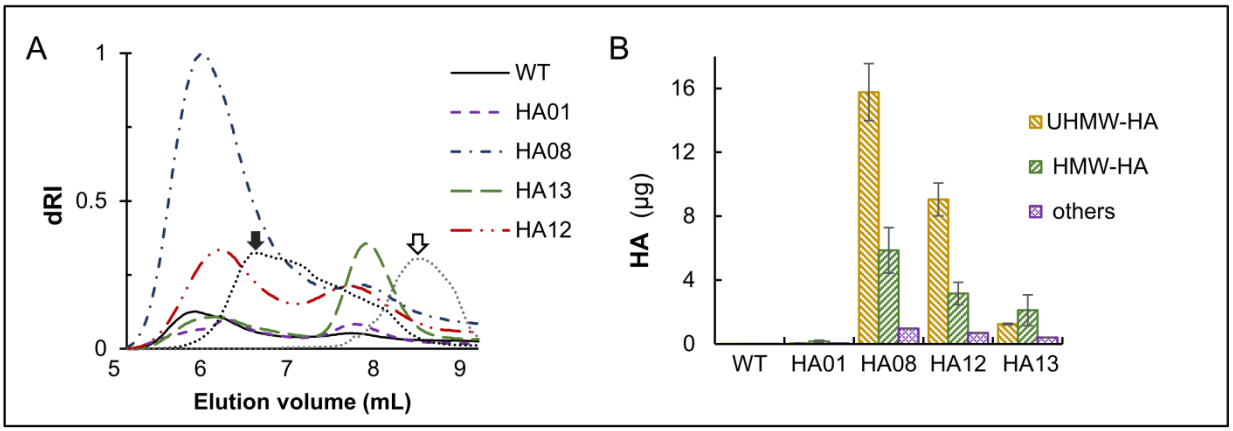

Figure 5. Size estimation of HA polymers from different strain by HPLC-SEC. **A.** Chromatograms of released polymers from different HA producing strains. Black filled arrow: commercial HA (molecular mass 2-2.2MDa); black outlined arrow: PEG polymer standard (molecular mass 1 MDa). **B.** HA content in each eluted peak. Peaks were eluted according to the intensity changes of dRI detector (elution times may vary between samples of different HA producing strains). Error bars represent standard deviation of technical duplicates. HA01: Δ*acsA*::$P_{cLac143}$-*pmHAS*; HA08: Δ*cesA*::Cm^R +Δ*acsA*::$P_{cLac143}$-*pmHAS*; HA12: Δ*glgA1*::P_{cpt}-*glmS-glmU-*Cm^R+Δ*acsA*::$P_{cLac143}$-*pmHAS*; HA13: Δ*glgA2*::P_{cpc560}-*tuaD-gtaB-*Km^R+Δ*acsA*::$P_{cLac143}$-*pmHAS*.

Supplementary materials

Table S1. List of primers used in this work.

Table S2. List of plasmids constructed in this work.

Table S3. Estimation of total fixed carbon partitioning to HA in different producing strains.

Figure S1. Introduction and expression of two different HA synthases into Syn7002.

Figure S2. Confocal microscopy images of Syn7002 cells expressing HA synthase.

Figure S3. Hyaluronidase digestion of cyanobacterial HA compared to commercial HA.

Figure S4. LC-MS/MS analysis of hyaluronidase digested samples from strain HA01 and commercial HA.

Figure S5. Effect of partial glycogen depletion on growth and HA production in Syn7002 strains, at 5 days post-IPTG induction.

Figure ~~S5~~S6. FTIR spectra of commercial HA and HPLC-purified HA produced by different strains.

5. References

[1] H. Niederholtmeyer, B.T. Wolfstadter, D.F. Savage, P.A. Silver, J.C. Way, Engineering cyanobacteria to synthesize and export hydrophilic products, Appl Environ Microb, 76 (2010) 3462-3466.

[2] C.J. Knoot, J. Ungerer, P.P. Wangikar, H.B. Pakrasi, Cyanobacteria: Promising biocatalysts for sustainable chemical production, J Biol Chem, 293 (2018) 5044-5052.

[3] G.D. Luan, X.F. Lu, Tailoring cyanobacterial cell factory for improved industrial properties, Biotechnol Adv, 36 (2018) 430-442.

[4] D.C. Ducat, J.C. Way, P.A. Silver, Engineering cyanobacteria to generate high-value products, Trends Biotechnol, 29 (2011) 95-103.

[5] A. Sarnaik, M.H. Abernathy, X.R. Han, Y.L. Ouyang, K. Xia, Y. Chen, B. Cress, F.M. Zhang, A. Lali, R. Pandit, R.J. Linhardt, Y.J. Tang, M.A.G. Koffas, Metabolic engineering of cyanobacteria for photoautotrophic production of heparosan, a pharmaceutical precursor of heparin, Algal Res, 37 (2019) 57-63.

[6] C.G. Boeriu, J. Springer, F.K. Kooy, L.A.M. van den Broek, G. Eggink, Production methods for hyaluronan, International Journal of Carbohydrate Chemistry, 2013 (2013) 1-14.

[7] N. Volpi, J. Schiller, R. Stern, L. Soltes, Role, metabolism, chemical modifications and applications of hyaluronan, Curr Med Chem, 16 (2009) 1718-1745.

[8] Hyaluronic Acid Market Size Worth USD 15.4 Billion by 2025, Grand View Research.

[9] L. Liu, Y.F. Liu, J.H. Li, G.C. Du, J. Chen, Microbial production of hyaluronic acid: current state, challenges, and perspectives, Microb Cell Fact, 10 (2011) 99-107.

[10] A. Zakeri, M.J. Rasaee, N. Pourzardosht, Enhanced hyluronic acid production in Streptococcus zooepidemicus by over expressing HasA and molecular weight control with Niscin and glucose, Biotechnol Rep (Amst), 16 (2017) 65-70.

[11] J.-H. Kim, S.-J. Yoo, D.-K. Oh, Y.-G. Kweon, D.-W. Park, C.-H. Lee, G.-H. Gil, Selection of a *Streptococcus equi* mutant and optimization of culture conditions for the production of high molecular weight hyaluronic acid, Enzyme and Microbial Technology, 19 (1996) 440-445.

[12] H.M. Yu, G. Stephanopoulos, Metabolic engineering of *Escherichia coli* for biosynthesis of hyaluronic acid, Metab Eng, 10 (2008) 24-32.

[13] Z.C. Mao, H.D. Shin, R. Chen, A recombinant *E. coli* bioprocess for hyaluronan synthesis, Appl Microbiol Biot, 84 (2009) 63-69.

[14] Y.N. Jia, J. Zhu, X.F. Chen, D.Y. Tang, D. Su, W.B. Yao, X.D. Gao, Metabolic engineering of *Bacillus subtilis* for the efficient biosynthesis of uniform hyaluronic acid with controlled molecular weights, Bioresource Technol, 132 (2013) 427-431.

[15] P. Jin, Z. Kang, P.H. Yuan, G.C. Du, J. Chen, Production of specific-molecular-weight hyaluronan by metabolically engineered *Bacillus subtilis* 168, Metab Eng, 35 (2016) 21-30.

[16] B. Widner, R. Behr, S. Von Dollen, M. Tang, T. Heu, A. Sloma, D. Sternberg, P.L. DeAngelis, P.H. Weigel, S. Brown, Hyaluronic acid production in *Bacillus subtilis*, Appl Environ Microb, 71 (2005) 3747-3752.

[17] Z.C. Mao, R.R. Chen, Recombinant synthesis of hyaluronan by *Agrobacterium sp.*, Biotechnol Progr, 23 (2007) 1038-1042.

[18] M.H. Abernathy, J. Yu, F. Ma, M. Liberton, J. Ungerer, W.D. Hollinshead, S. Gopalakrishnan, L. He, C.D. Maranas, H.B. Pakrasi, D.K. Allen, Y.J. Tang, Deciphering cyanobacterial phenotypes for fast photoautotrophic growth via isotopically nonstationary metabolic flux analysis, Biotechnol Biofuels, 10 (2017) 273-285.

[19] B.W. Abramson, J. Lensmire, Y.T. Lin, E. Jennings, D.C. Ducat, Redirecting carbon to bioproduction via a growth arrest switch in a sucrose-secreting cyanobacterium, Algal Res, 33 (2018) 248-255.

[20] C. Zhao, Z.K. Li, T. Li, Y.J. Zhang, D.A. Bryant, J.D. Zhao, High-yield production of extracellular type-I cellulose by the cyanobacterium *Synechococcus* sp PCC 7002, Cell Discov, 1 (2015) 15004-15015.

[21] P. Flombaum, J.L. Gallegos, R.A. Gordillo, J. Rincon, L.L. Zabala, N. Jiao, D.M. Karl, W.K. Li, M.W. Lomas, D. Veneziano, C.S. Vera, J.A. Vrugt, A.C. Martiny, Present and future global distributions of the marine Cyanobacteria Prochlorococcus and Synechococcus, Proc Natl Acad Sci U S A, 110 (2013) 9824-9829.

[22] D.S. Snyder, B. Brahamsha, P. Azadi, B. Palenik, Structure of compositionally simple lipopolysaccharide from marine synechococcus, J Bacteriol, 191 (2009) 5499-5509.

[23] I. Stewart, P.J. Schluter, G.R. Shaw, Cyanobacterial lipopolysaccharides and human health - a review, Environ Health, 5 (2006) 7-29.

[24] M. Klemenčič, A.Z. Nielsen, Y. Sakuragi, N.U. Frigaard, H. Čelešnik, P.E. Jensen, D. M., Synthetic biology of cyanobacteria for production of biofuels and high-value products, in: C. Gonzalez-Fernandez, R. Muñoz (Eds.), Microalgae-Based Biofuels and Bioproducts, Woodhead Publishing, 2017, pp. 305-325.

[25] T.T. Selao, A. Wlodarczyk, P.J. Nixon, B. Norling, Growth and selection of the cyanobacterium *Synechococcus sp.* PCC 7002 using alternative nitrogen and phosphorus sources, Metab Eng, 54 (2019) 255-263.

[26] M.B. Begemann, E.K. Zess, E.M. Walters, E.F. Schmitt, A.L. Markley, B.F. Pfleger, An organic acid based counter selection system for cyanobacteria, Plos One, 8 (2013) 76594-76605.

[27] J. Zhou, H.F. Zhang, H.K. Meng, Y. Zhu, G.H. Bao, Y.P. Zhang, Y. Li, Y.H. Ma, Discovery of a super-strong promoter enables efficient production of heterologous proteins in cyanobacteria, Sci Rep-Uk, 4 (2014) 4500-4505.

[28] A.L. Markley, M.B. Begemann, R.E. Clarke, G.C. Gordon, B.F. Pfleger, Synthetic biology toolbox for controlling gene expression in the cyanobacterium *Synechococcus* sp. strain PCC 7002, Acs Synth Biol, 4 (2015) 595-603.

[29] M. Kostylev, A.E. Otwell, R.E. Richardson, Y. Suzuki, Cloning should be smple: *Escherichia coli* DH5 alpha-mediated assembly of multiple DNA fragments with short end fomologies, Plos One, 10 (2015) 1371-1385.

[30] A.M. Ruffing, Improved Free Fatty Acid Production in Cyanobacteria with *Synechococcus sp. PCC 7002* as Host, Frontiers in bioengineering and biotechnology, 2 (2014) 17-26.

[31] L.N. Liu, S.J. Bryan, F. Huang, J.F. Yu, P.J. Nixon, P.R. Rich, C.W. Mullineaux, Control of electron transport routes through redox-regulated redistribution of respiratory complexes, P Natl Acad Sci USA, 109 (2012) 11431-11436.

[32] T.T. Selao, L.F. Zhang, J. Knoppova, J. Komenda, B. Norling, Photosystem II assembly steps take place in the thylakoid membrane of the cyanobacterium *Synechocystis sp* PCC6803, Plant Cell Physiol, 57 (2016) 95-104.

[33] T.M.M. Bernaerts, L. Gheysen, C. Kyomugasho, Z.J. Kermani, S. Vandionant, I. Foubert, M.E. Hendrickx, A.M. Van Loey, Comparison of microalgal biomasses as functional food ingredients: Focus on the composition of cell wall related polysaccharides, Algal Res, 32 (2018) 150-161.

[34] R. Dephilippis, M.C. Margheri, E. Pelosi, S. Ventura, Exopolysaccharide Production by a Unicellular Cyanobacterium Isolated from a Hypersaline Habitat, J Appl Phycol, 5 (1993) 387-394.

[35] Z.Q. Zhang, J. Xie, J. Liu, R.J. Linhardt, Tandem MS can distinguish hyaluronic acid from N-acetylheparosan, J Am Soc Mass Spectr, 19 (2008) 82-90.

[36] A.V. Kuhn, K. Raith, V. Sauerland, R.H.H. Neubert, Quantification of hyaluronic acid fragments in pharmaceutical formulations using LC-ESI-MS, J Pharmaceut Biomed, 30 (2003) 1531-1537.

[37] S. Haserodt, M. Aytekin, R.A. Dweik, A comparison of the sensitivity, specificity, and molecular weight accuracy of three different commercially available Hyaluronan ELISA-like assays, Glycobiology, 21 (2011) 175-183.

[38] S.G. Ball, M.K. Morell, From bacterial glycogen to starch: understanding the biogenesis of the plant starch granule, Annu Rev Plant Biol, 54 (2003) 207-233.

[39] M.L. Fisher, R. Allen, Y.Q. Luo, R. Curtiss, Export of extracellular polysaccharides modulates adherence of the cyanobacterium *Synechocystis*, Plos One, 8 (2013) 74514-74523.

[40] Y. Xu, L.T. Guerra, Z.K. Li, M. Ludwig, G.C. Dismukes, D.A. Bryant, Altered carbohydrate metabolism in glycogen synthase mutants of *Synechococcus* sp strain PCC 7002: Cell factories for soluble sugars, Metab Eng, 16 (2013) 56-67.

[41] J.D. de Oliveira, L.S. Carvalho, A.M.V. Gomes, L.R. Queiroz, B.S. Magalhaes, N.S. Parachin, Genetic basis for hyper production of hyaluronic acid in natural and engineered microorganisms, Microb Cell Fact, 15 (2016) 119-137.

[42] J.W. Chwa, W.J. Kim, S.J. Sim, Y. Um, H.M. Woo, Engineering of a modular and synthetic phosphoketolase pathway for photosynthetic production of acetone from CO_2 in *Synechococcus elongatus* PCC 7942 under light and aerobic condition, Plant Biotechnol J, 14 (2016) 1768-1776.

[43] A.J. De Porcellinis, H. Norgaard, L.M.F. Brey, S.M. Erstad, P.R. Jones, J.L. Heazlewood, Y. Sakuragi, Overexpression of bifunctional fructose-1,6-bisphosphatase/sedoheptulose-1,7-bisphosphatase leads to enhanced photosynthesis and global reprogramming of carbon metabolism in *Synechococcus sp* PCC 7002, Metab Eng, 47 (2018) 170-183.

Highlights

- Cyanobacteria are promising hosts for carbon-neutral hyaluronic acid (HA) production
- Two heterologous HA synthases are active in a marine cyanobacterium strain
- Cellulose synthase knock-out improves both HA titer and molecular mass
- Addition of UDP-GlcNAc or UDP-GlcUA synthesis enzymes increases HA production
- Combination of UDP-GlcNAc synthesis with glycogen depletion boosts HA yields

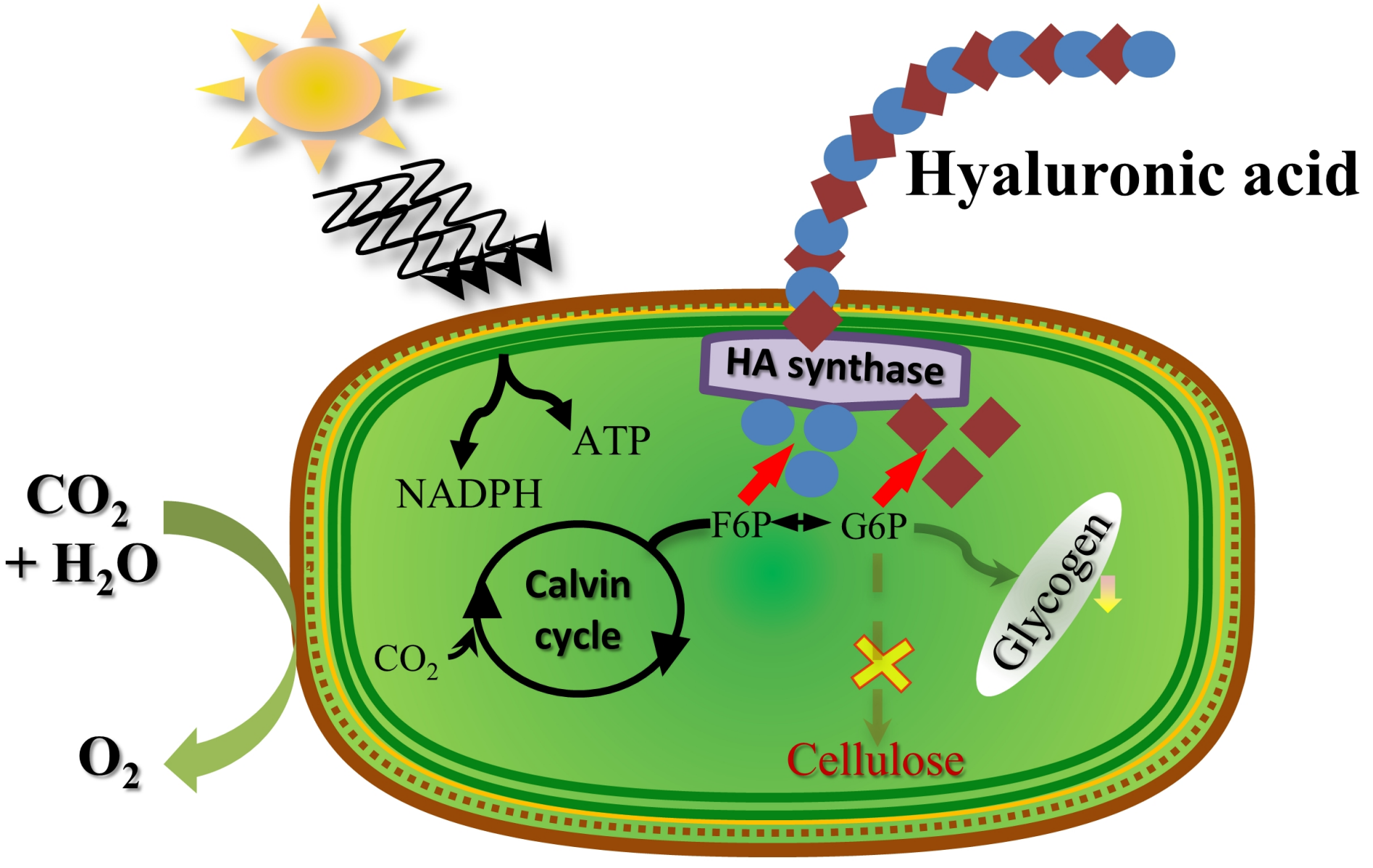
Hyaluronic acid
HA synthase
ATP
NADPH
CO_2
+ H_2O
O_2
F6P
G6P
Calvin cycle
CO_2
Glycogen
Cellulose

Photosynthetic conversion of CO_2 to hyaluronic acid by engineered strains of the cyanobacterium *Synechococcus* sp. PCC 7002

Lifang Zhang [a], Tiago Toscano Selão [a], Peter J. Nixon [a, b] and Birgitta Norling [a]

[a] School of Biological Sciences, Nanyang Technological University, Singapore

[b]Sir Ernst Chain Building-Wolfson Laboratories, Department of Life Sciences, Imperial College London, S. Kensington Campus, London, SW7 2AZ, UK

Corresponding author: Birgitta Norling, School of Biological Sciences, Nanyang Technological University, Singapore**;** email: ibnorling@ntu.edu.sg

Abstract

Hyaluronic acid (HA), consisting of alternating N-acetylglucosamine and glucuronic acid units, is a natural polymer with diverse cosmetic and medical applications. Currently, HA is produced by overexpressing HA synthases from gram-negative *Pasteurella multocida* (encoded by *pmHAS*) or gram-positive *Streptococcus equisimilis* (encoded by *seHasA*) in various heterotrophic microbial production platforms. Here we introduced these two different types of HA synthase into the fast-growing cyanobacterium *Synechococcus* sp. PCC 7002 (Syn7002) to explore the capacity for producing HA in a photosynthetic system. Our results show that both HA synthases enable Syn7002 to produce HA photoautotrophically, but that overexpression of the soluble HA synthase (PmHAS) is less deleterious to cell growth and results in higher production. Genetic disruption of the competing cellulose biosynthetic pathway increased the HA titer by over 5-fold (from 14 mg/L to 80 mg/L) and the relative proportion of HA with molecular mass greater than 2 MDa. Introduction of *glmS* and *glmU*, coding for enzymes involved in the biosynthesis of the precursor UDP-N-acetylglucosamine, in combination with partial glycogen depletion, allowed photosynthetic production of 112 mg/L of HA in 5 days, an 8-fold increase in comparison to the initial PmHAS expressing strain. Addition of *tuaD* and *gtaB* (coding for genes involved in UDP-glucuronic acid biosynthesis) also improved the HA yield, albeit to a lesser extent. Overall our results have shown that cyanobacteria hold promise for the sustainable production of pharmaceutically important polysaccharides from sunlight and CO_2.

Keywords

Cyanobacteria; metabolic engineering; hyaluronic acid; photoautotrophic production

Abbreviations

WT – wild type

GFP – Green Fluorescent Protein

RBS – ribosome binding site

UDP– uridine diphosphate

IPTG– Isopropyl β-D-1-thiogalactopyranoside

PEG– polyethylene glycol

1. Introduction

Cyanobacteria are gaining attention as hosts for photosynthetic production of high-value molecules due to their easier genetic manipulation in comparison to other photosynthetic systems and favourable growth rates [1, 2]. Metabolic engineering of cyanobacteria has successfully led to the production of a wide range of industrially relevant products [3, 4]. However, apart from a very recent report on the production of heparosan [5], the use of cyanobacteria to produce pharmaceutically important polysaccharides remains relatively unexplored.

Hyaluronic acid (HA) is a unique biopolymer composed of alternating β-1,3-N-acetyl glucosamine and β-1,4-glucuronic acid disaccharide units [6]. Its distinctive moisturizing and viscoelastic properties, coupled to a lack of immunogenicity and toxicity, have led to a wide range of proven and marketed applications for HA within the cosmetic and biomedical industries [7]. The global HA market was valued at USD 7.2 billion in 2016 and is expected to reach USD 15.4 billion by 2025 [8], with most of the commercial HA being either isolated from animal sources, such as rooster combs, or made by microbial fermentation [9]. While production by modified group C *Streptococcus* strains under specific growth conditions can reach 6-7 g/L in fed-batch fermentation [10, 11], it has several drawbacks, such as the potential problem of contamination by endotoxins. The increased demand for HA and arising safety concerns have led researchers to use synthetic biology and metabolic engineering approaches to develop alternative sources of HA production.

Two types of HA synthase, catalyzing the final HA synthesis step, are commonly used in metabolic engineering efforts, most commonly the enzymes PmHAS from *Pasteurella multocida* and SeHasA (or SzHasA) from *Streptococcus* species. Successful HA production was previously demonstrated in genetically modified non-pathogenic *Bacillus subtilis* and *Escherichia coli* strains overexpressing different HA synthases, along with the relevant

precursor synthesis enzymes [12-17]. Although HA titers in these modified strains are promising, with some being used in industrial scale processes [16], their production is completely based on fermentative processes, requiring the input of substantial amounts of carbon feedstocks, such as glucose or sucrose. On the other hand, photosynthetic bio-manufacturing processes for the sustainable and economic production of value-added chemicals are an increasingly promising solution to these issues. Cyanobacteria can naturally convert CO_2 into diverse carbohydrates and have high intracellular nucleotide sugar pool sizes [18]. Additionally, some strains have already been engineered to produce and excrete either soluble sugars (such as sucrose [19]) or polysaccharides, e.g. crystalline cellulose [20] or heparosan [5].

Synechococcus sp. are one of the major groups of marine cyanobacteria and its representatives play an important role in the global food chain and carbon cycle [21]. While these strains are also known to produce lipopolysaccharides (LPS), the immune response to different *Synechococcus* sp. LPS is either negative [22] or at least 3 orders of magnitude below that of other gram-negative bacteria [23], and they are therefore considered as safe hosts for biotechnological applications [24]. In this study, we aimed to engineer *Synechococcus* sp. PCC 7002 (hereafter Syn7002), a fast growing and robust chassis strain, into a photosynthetic HA production system, thus demonstrating that cyanobacteria have the potential to become viable and safe alternatives for the sustainable production of biomedically relevant polysaccharides.

2. Material and Methods

2.1. Strains and culture conditions

Wild-type *Synechococcus* sp. PCC 7002 (a kind gift from Donald Bryant, Pennsylvania State University, USA) and all derivative strains were grown in medium AD7 [25] and supplemented with antibiotics as required, namely chloramphenicol (10 μg/mL) and/or

kanamycin (100 μg/mL). Liquid cultures and plates were grown in an atmosphere of CO_2-enriched (1% (v/v)) air, under continuous illumination (300 μmol photons m^{-2} s^{-1}) at 38 °C, as previously described [25]. Growth was monitored by measuring OD_{730} in a plate reader (Hidex Sense, Hidex) and utilizing an in-house generated 70-point calibration curve (R^2=0.9818) converting OD_{730} in the plate reader to that measured using a 1 cm light path table top spectrophotometer (Cary 300Bio, Varian), using AD7 as blank. Dry cell weight at 5 days was measured as previously described [25]. All growth measurements were performed using biological triplicates (n=3). To test HA production, cultures were pre-adjusted to an OD_{730}=1, induced by addition of 1 mM IPTG, and samples collected at the time points indicated. Cell pellets and supernatants were stored at -20 °C until further use.

2.2. Cyanobacterial strain construction

Genes encoding two HA synthases, *pmHAS* and *seHasA,* (the latter with a C-terminal FLAG tag), as well as *B. subtilis* genes encoding UDP-glucose dehydrogenase (*tuaD*), UDP-glucose pyrophosphorylase (*gtaB*), and the *E. coli* genes encoding glutamine amidotransferase (*glmS*) and acetyl-CoA acetyltransferase/pyrophosphorylase (*glmU*, a homologue of *gcaD* in *B. subtilis*) were codon-optimized for Syn7002 and synthesized by GenScript (Hong Kong). The expression of both HA synthase genes was controlled by an IPTG inducible promotor, $P_{cLac143}$, based on plasmid *pAcsA*-$P_{cLac143}$-*YFP* (a kind gift from Brian Pfleger, University of Wisconsin-Madison, USA) [26]. The *tuaD* and *gtaB* genes were synthesized as an artificial operon, under control of the strong constitutive P_{cpc560} promoter [27], with a second artificial operon containing *glmS* and *glmU*, controlled by the strong constitutive P_{cpt} promoter [28]. In all cases, the strong AGGAGA RBS sequence was utilized, with a random 8 bp DNA sequence between RBS and the initial ATG codon [28]. All enzymes utilized were purchased from NEB unless otherwise specified and all primers used are listed in Table S1. DNA fragments were PCR amplified with Q5 DNA polymerase, purified using the EZ-10 Spin Column PCR Products

Purification Kit (Bio-Basic, Canada) and assembled either using the pEASY-Uni Seamless Cloning and Assembly Kit (TransGen Biotech, China), following manufacturer's instructions, or by *E. coli* mediated assembly [29]. Supercompetent *E. coli* cells (Stellar, TaKaRa) were used for all cloning steps and were grown in LB medium supplemented with antibiotics as required - ampicillin (100 µg/mL), chloramphenicol (25 µg/mL) or kanamycin (50 µg/mL). The sequence of all constructed plasmids (Table S2) was confirmed by Sanger sequencing. Syn7002 transformation was performed according to standard protocols [30]. Full genomic segregation in modified strains was confirmed by colony PCR using specific primers. A list of all strains generated in this work is presented in Table 1.

2.3. Fluorescence microscopy and western blot

Preparation of Syn7002 cells for confocal microscopy was performed as described earlier [31]. Essentially, cells from IPTG-induced cultures were collected and blotted on a 1% agarose gel pad (prepared with AD7 medium) for image analysis. Laser scanning confocal microscopy was performed using an LSM710 (Carl Zeiss), with a 1.4 NA Plan-Apo 60x oil immersion lens used as an objective at a zoom factor of 10 and excitation at 488 nm. Image analysis was carried out using the Zen software (Carl Zeiss, version 2.3). Cell size estimates were made using the measuring tool in the Zen software and calculating averages and standard deviations from 15-20 cells from each strain, imaged at the same magnification.

Whole-cell lysates were isolated as previously described and subjected to western blot analysis [32]. 10 µg total proteins were separated on 12% precast SDS-PAGE gels (BioRad), transferred onto PVDF membranes and probed with primary antibodies raised in rabbit against a synthetic PmHAS peptide (NDNDLKSMNVKGAS, amino acids 860 to 874, prepared by GenScript, Hong Kong) and/or a monoclonal mouse anti-FLAG M2 antibody (F3165, Sigma-Aldrich).

2.4. Cyanobacterial HA preparation and quantification by ELISA

HA production by engineered Syn7002 strains was routinely assessed by measuring the HA released into the growth medium at the indicated time points. Cells were collected by centrifugation (3000 g, 10 min, room temperature) and the cleared supernatant was used to assay HA levels. To concentrate HA from cyanobacterial cultures, 3 volumes of ice-cold ethanol were added to the cleared supernatants and the resulting pellets were dried in air and re-suspended in deionised H_2O for further use [33]. To evaluate the HA secretion ability of different strains, released HA (R-HA), capsular HA (bound to the cell surface, CPS-HA) and intracellular HA (intra-HA) were isolated according to previously described methods [12, 34], with whole cell lysates for intra-HA quantification prepared according to Selão et al [32]. HA quantification was performed using a Hyaluronan Quantikine ELISA Kit (DHYAL0, R&D systems, USA), following the manufacturer's instructions, either directly or by diluting samples with AD7 prior to quantification, and absorbance of the ELISA strips was measured using the Hidex Sense plate reader.

2.5. Characterization of HA by HPLC, LC-MS/MS and FTIR

Cyanobacterial HA was further analysed using an UFLC Prominence (Shimadzu, Japan) equipped with a size-exclusion chromatography column (Shodex OHpak, SB806 M HQ, 8.0 mm×300 mm, 13µm particle size, Shimadzu), coupled to a UV detector (Shimadzu, Japan) and a differential refractive index detector (dRI, Optilab rEX, Wyatt Technology, USA). The mobile phase was a 0.1 M NaCl solution and all chromatography runs were performed at 0.5 mL/min. Samples were filtered through 0.2 µm Whatman Puradisc 13 syringe filters (GE Healthcare, USA) prior to injection and 150 µL were used in each run. Chromatography data was recorded and analyzed by the ASTRA software (version 5.3, Wyatt Technology, USA). All peaks detected by the dRI detector were collected and saved at -20 °C until further use. The molecular mass of detected peaks was estimated by comparison to the elution times of PEG

analytical standard (ReadyCal Set, #02393, Sigma-Aldrich) and of commercial HA with known molecular mass (2-2.2 MDa, #51967, Sigma-Aldrich).

LC-MS/MS was used to characterize the forming units of HA polymer produced by the PmHAS-expressing strains following hyaluronidase digestion. HPLC-purified sample was precipitated using ethanol as described above, and subjected to hyaluronidase (#H3506, Sigma-Aldrich) digestion according to manufacturer's instructions. After confirmation of complete digestion using both the HA ELISA assay and HPLC, the resulting fragments were analyzed by LC-MS/MS, using a Xevo-TQ-S (Waters, Milford, USA) mass spectrometry system, coupled to an ACQUITY UPLC system (Waters) with a 2.1mm x 100mm HSS T3 Column, 1.8µm particle size (Waters), as previously described [35]. Cyanobacterial HA from HPLC eluted peaks was also subjected to Fourier transform infrared spectroscopy (FTIR) analysis after precipitation with cold ethanol. 10 µL samples were evenly spotted on a horizontal ZnSe ATR element (Pike Technologies) and dried under a stream of dry, CO_2-free air. The respective spectra (average from 200 scans at 4 cm^{-1} resolution) were recorded between 4000-650 cm^{-1} using an FTIR Nicolet Nexus 470 instrument (Thermo Scientific), purged with dry, CO_2-free air and equipped with an MCT/A detector cooled with liquid nitrogen.

3. Results and Discussion

3.1. Overexpression of HA synthase in Syn7002

As with all cyanobacteria sequenced so far, Syn7002 lacks homologues of the known HA synthases and is not known to naturally produce HA. However, an analysis of its predicted metabolic network (using the KEGG database) suggests that this organism has all the enzymes required to synthesize the two HA precursor molecules, UDP-GlcUA and UDP-GlcNAc (Fig. 1). Both of these UDP-sugars, as well as their precursors, are used for cyanobacterial cell wall

biosynthesis and could theoretically be redirected to the biosynthesis of HA or similar polysaccharides [5].

We used a previously described IPTG-inducible expression system (the $P_{cLac143}$ promoter system [28]) to regulate the expression of PmHAS or SeHasA, and integrated the two respective genes at the *acsA* locus of Syn7002 (Fig. 2A). Fully segregated strains (HA01 harboring *pmHAS* and HA03 containing *seHasA*), as well as C-terminal GFP-tagged versions (HA02 and HA04 respectively), were confirmed by colony PCR (Fig. 2B). Immunoblotting experiments confirmed that expression of both HA synthases was induced upon IPTG addition (Fig. 2C), with overexpression of PmHAS and SeHasA resulting in the appearance of either a 110 kDa or a 49 kDa protein, respectively. Overexpression of either HA synthase impacted cell growth, with SeHasA having a more severe effect (Fig. S1A).

HA synthase activity in these strains was evaluated by quantifying HA present in the medium after IPTG induction using a specific ELISA Kit, which uses a specific HA-binding protein for recognition and quantification of HA with molecular mass higher than 35 kDa [37]. While WT cultures produced no detectable HA, strains expressing either of the HA synthases produced moderate amounts of HA upon induction. For strain HA01, the HA concentration in the medium increased from 9.8±0.85 mg/L (at 5 days post-induction) to 31.9±4.0 mg/L (at 10 days post-induction) while strain HA03 had an overall lower HA production in comparison to the HA01 strain (Fig. 2D). However, as the higher HA concentration at 10 days was linked to a decline in the cell density of the culture, all subsequent HA production experiments were performed with cell cultures at an earlier growth phase (up to 5 days post-induction).

To understand better the reasons behind the low productivity of strain HA03 (expressing the integral membrane SeHasA synthase), the location of both enzymes was studied by adding a C-terminal superfolder-GFP (sfGFP) tag. This tag did not negatively affect HA synthesis activity, with similar amounts of HA detected in the growth medium 5 days post-IPTG

induction (Fig. S1B). Confocal microscopy revealed that cells expressing sfGFP-tagged derivatives of PmHAS (HA02) and SeHasA (HA04) were larger than WT, with SeHasA expression having a more pronounced effect (Fig. S2). While overexpressing sfGFP alone in Syn7002 resulted in cells with average dimensions of 1.9±0.1 μm×1.3±0.1 μm (length × width), accumulation of PmHAS-sfGFP in strain HA02 lead to a slight increase in cell size (2.7±0.7 μm×1.7±0.1 μm) and accumulation of SeHasA-sfGFP in strain HA04 significantly increased cellular dimensions (4.1±0.9 μm×2.3±0.2 μm). sfGFP fluorescence was concentrated in the cytoplasm of HA02 cells but mostly found in random patches in HA04. Thylakoid membranes in HA04 cells also seemed distorted, possibly by mistargeting of integral membrane protein SeHasA or due to accumulation of HA in the lumenal space. Consequently, all further engineered strains used PmHAS, since this soluble HA synthase was more benign and more productive than its integral counterpart.

3.2. Characterization of HA produced by PmHAS in Syn7002

In addition to the specific ELISA assay, we employed several alternative methods to positively identify the polymers produced upon expressing PmHAS. Strain HA01 was used to isolate released cyanobacterial polysaccharides by ethanol precipitation from culture supernatants 5 days after IPTG induction. The obtained material (HA01-HA) was analyzed by hyaluronidase digestion, HPLC-SEC, and LC-MS/MS. Hyaluronidase digestion of HA01- HA, similarly to that of commercial HA, resulted in a loss of detection by the ELISA assay and a shift to much smaller polymer sizes, as detected by HPLC-SEC (Fig. S3). LC-MS/MS analysis of the hyaluronidase-digested samples identified the typical HA disaccharide with m/z 395.7 and tetrasaccharide with m/z 774.9 both in the digested HA01-HA sample and the commercial HA control (Fig. S4), further verifying the identity of the produced polymer.

3.3. Cellulose removal benefits HA production

The biosynthesis of HA in our modified Syn7002 strains relies solely on intermediates derived from photosynthetic carbon fixation (see Fig. 1), which are also commonly used by cells for the generation of internal glycogen storage granules [38] or are converted to UDP-Glucose (UDP-Glc) for synthesis of cell wall components, such as cellulose or other types of polysaccharide [39]. The carbon flux towards HA synthesis is therefore potentially limited by these other pathways. As the biosynthesis pathways involved in cell wall polysaccharides have not been fully characterized in Syn7002, we focused on the possible effect of blocking cellulose synthesis or lowering the glycogen level on HA production. Therefore, several deletion mutants were constructed to investigate their influence on HA production (Fig. 3A).

Deletion of either of the two glycogen synthase genes (*glgA1* and *glgA2*) had only minor effects on HA production in comparison to the HA01 strain (Fig. S5), even though each deletion should increase glucose-1-phosphate pools and decrease glycogen biosynthesis by ≈50% [40]. The limited effects of partial glycogen depletion on HA production may imply that either Glc-1-P could not be efficiently converted to UDP-GlcUA or the limiting step for HA production might be related to the synthesis of the other precursor, UDP-GlcNAc. Cellulose, an insoluble polysaccharide that is also produced by some cyanobacteria, is synthesized in Syn7002 by a cellulose synthase (CesA) the deletion of which was shown to be essential for high-level cellulose production in engineered Syn7002 [20]. Our results show that overexpression of PmHAS in strain HA08 (a *cesA* knock-out background) led to a mild growth impairment in comparison to both WT and the basic HA01 strain, which was offset by substantially improved HA production, reaching 80.4±4.2 mg/L on the 5th day post-induction (in comparison to 14.8±2.0mg/L in HA01, Fig. 4A). This marked improvement in HA production upon disruption of cellulose synthesis may be due to a higher flux from UDP-glucose to UDP-GlcUA, one of the HA precursors, as mentioned above. On the other hand, as cellulose was found to form a laminar layer in Syn7002, located in the vicinity of the

peptidoglycan layer [20], there is also the possibility that endogenous cellulose removal may facilitate excretion of HA by removal of a physical barrier.

3.4. HA yield is improved by overexpression of enzymes involved in precursor biosynthesis

A commonly utilized strategy in other bacterial strains engineered for HA production is to strengthen the biosynthesis of the precursors UDP-GlcUA and/or UDP-GlcNAc [41]. Studies using recombinant strains of *B. subtilis* overexpressing either SeHasA or PmHAS have shown that UDP-glucuronic acid (UDP-GlcUA) biosynthesis can be a limiting step for production of HA [14, 16], with co-overexpression of PmHAS and TuaD-GtaB allowing a maximum titer of 6.8 g/L. Conversely, the co-overexpression of PmHAS with GcaD (a homologue of GlmU), involved in synthesis of UDP-GlcNAc, produced very low molecular mass HA and improved HA titer to a lesser extent (2.4 g/L) [14]. A similar strategy also allowed modified *E. coli* strains to reach a final titer of 3.8 g/L in a fed-batch reactor [13]. Although most of the enzymes involved in HA precursor biosynthesis have predicted homologs in cyanobacteria (as shown in Fig. 1), the expression, functionality and regulation of those Syn7002 gene products have so far not been studied and it was therefore preferable to manipulate precursor biosynthesis by expressing heterologous enzymes.

An artificial operon to improve UDP-GlcNAc biosynthesis, P_{cpt}-*glmS*-*glmU*, was introduced into either the *glpK* neutral locus in strain HA11 [26] or the *glgA1* site in strain HA12 (Fig. 3). HA production increased in both strains, to 111.9±10.6 mg/L in HA12 and 35.9±5.5 mg/L in HA11 (Fig. 4A), demonstrating that enhanced biosynthesis of UDP-GlcNAc improves HA yields in Syn7002, an effect magnified when glycogen synthesis was simultaneously inhibited. Although HA production was not improved by merely deleting *glgA1* (or *glgA2*), the combination of lower glycogen biosynthesis with increasing synthesis of the precursor UDP-GlcNAc did successfully divert carbon flow to the final product, HA. Separately, to increase

UDP-GlcUA precursor pools, the P_{cpc560}-*tuaD-gtaB* operon was introduced into the other glycogen synthase locus (*glgA2*) of Syn7002 in strain HA13 (Fig. 3). HA production (29.3±9.5 mg/L) improved in comparison to HA01, albeit to a lesser extent than in strain HA12 (Fig. 4A). Interestingly, overexpression of UDP-GlcUA-related enzymes in Syn7002 did not influence HA titers as strongly as in heterotrophic organisms [14, 16, 17]. As heterologous HA production diverts intermediates away from cell wall biogenesis, growth was affected by HA production, with higher HA titers generally resulting in lesser growth (lower OD_{730}), particularly in the case of strain HA12, which had both the lowest cell density and the highest titer (Fig. 4A).

3.5. Released HA is only a minor fraction of the total production

As the mechanism for HA secretion in PmHAS-utilizing bacterial strains is unknown, we tested the excretion efficiency of producing strains by quantifying HA isolated from different locations. We found that in all the strains tested large amounts of HA were retained within the cells, ranging from 42% to roughly 88%. Strain HA12, with the UDP-GlcNAc pathway enhanced, was able to release a higher portion of HA into the medium, however the vast majority of the product (about 60%) was still trapped within the cell (Fig. 4B). Interestingly, strain HA08 with cellulose removed had the highest amount of capsular HA among all the strains. Nearly 50% of the total HA production for strain HA08 was found attached to the cell surface (Fig. 4B). One possible explanation is that removal of the cellulose layer facilitates secretion of HA, even if it is not completely released from the cell surface. In light of these results, it seems clear that, even though all the generated strains improved their HA production capabilities, secretion and release of such large polymer is still a major bottleneck. Clearly, the mechanism responsible for polysaccharide (HA) excretion in cyanobacteria is unable to efficiently export the large amount of HA produced by the engineered strains, which may also be one of the causes for the growth defects observed.

Total HA production of these strains was calculated by summing up the values obtained from different fractions and photosynthetic CO_2 partitioning was estimated according to measured dry cell biomass, the carbon fraction in HA of 44.4% and assuming that total cellular carbon is 51.3% of cell biomass (as previously described [42]). Strain HA12 has the highest carbon partitioning efficiency (≈25%), a substantial increase in comparison to strain HA01 (converting <2% of fixed carbon to HA). Overexpression of GlmS and GlmU most likely diverts carbon flow from the primary photosynthetic intermediate fructose-6-phosphate, to synthesize UDP-GlcNAc, resulting in comparatively better carbon partitioning (Fig. 4B and Table S3), though at the expense of cell growth (Fig. 4A). Strain HA08 (with *cesA* deleted) showed a similar CO_2 partitioning to HA as strain HA13 (roughly 16%), but with a better growth performance, which may be more suitable for sustainable production of HA.

3.6. The molecular weight of excreted HA varies with different pathway modifications

Size-exclusion chromatography was used to characterize the molecular mass of the excreted polymers produced by the different strains, using 2-2.2 MDa commercial HA and 1 MDa PEG polymers as standards. All samples from the different strains had two major peaks, one with a molecular mass greater than 2-2.2 MDa and a smaller one with mass greater than 1 MDa, referred to as "UHMW-HA" and "HMW-HA" respectively (Fig. 5). These peaks were further analyzed by HA quantification (Fig. 5B) and FTIR (Fig. S6). The quantification of the HA content of each eluted peak generally fits with the peak intensity shown by the chromatography spectra, indicating that the introduced modifications, while possibly influencing precursor levels, resulted in changes to the size of produced HA. As shown in Fig. 5, strains HA08 and HA12 had a higher proportion of the UHMW-HA, whereas strains HA01 and HA13 strains excreted mainly HMW-HA. The reason for this is unclear but might be related to the different regulation mechanisms at the level of polymerization and secretion, as previously seen in engineered *B. subtilis* strains [14]. FTIR spectra for the major chromatography peaks isolated

from the HA-producing strains, but not from WT Syn7002, were very similar to that of commercial HA (Fig. S6), again confirming the identity of the produced polymers.

4. Conclusions

This work shows that cyanobacteria are promising hosts to produce biomedically-relevant sugar polymers solely by photosynthesis, paving the way for the sustainable production of hyaluronic acid. Heparosan was recently shown to be produced by heterologous expression of a heparosan synthase in *Synechococcus* sp. PCC 7942, although with an extremely low yield (3 μg/L) [5]. The best performing strain in the current report (HA12) shows a several thousand-fold improvement in comparison to the heparosan-producing strains, perhaps owing to codon-optimization of the introduced enzymes, more robust growth of our cyanobacterial host in comparison to *Synechococcus* sp. PCC7942 and iterative metabolic engineering. HA production was successfully improved by using different strategies, such as deleting the endogenous cellulose synthase gene and overexpressing precursor biosynthesis enzymes and, especially in the case of the UDP-GlcNAc pathway, combining precursor biosynthesis with glycogen depletion was particularly beneficial for production, though at the cost of growth performance.

Even if these results are encouraging, several issues still remain to be solved before cyanobacteria can compete with the yields observed in heterotrophic hosts. Increasing the photosynthetic performance of cyanobacteria is a commonly used strategy for improved yield, as this could improve up-stream precursor pools for HA synthesis and other metabolites [43]. PmHAS-mediated HA secretion may be further improved by down-regulating other competing pathways (such as O-antigen or peptidoglycan synthesis), which might also remove physical barriers further improving HA excretion.

As environmentally conscious processes become increasingly relevant in relation to the mitigation of climate change, the development of efficient engineered cyanobacterial cell

factories could allow biopolymer production without competing for food-grade materials, arable land or freshwater resources, thus contributing to a more sustainable bio-economy.

Acknowledgements

This work was supported by NTU grants M4080306 to BN and M4081714 to PJN. The authors would like to thank Dr. Wahyu Surya (SBS, NTU) for assistance with the size-exclusion chromatography analysis of samples and Associate Professor Jaume Torres (SBS, NTU) for access to his FTIR spectrometer. We would also like to thank the NTU Optical Microscopy for cell imaging analysis and NTU Phenomics Centre for LC-MS/MS analysis of HA fragments. The authors are grateful to Prof. Bertil Andersson for his constant support and encouragement and his pivotal role in establishing the CyanoSynBio@NTU laboratory.

Contributions

LZ, TTS, PJN and BN conceptualized and designed the present study. TTS performed the initial cloning of HA synthases in the expression vector, LZ performed all other strain engineering, cyanobacteria cultivation, production tests and product analysis. All authors contributed to data analysis, manuscript drafting and revision, agree to authorship and approve the final manuscript for submission.

Conflict of interest

Declarations of interest: none.

Tables and Figures

Table 1. Engineered cyanobacterial strains used for HA production in the study.

Strain name	Genotype	Characteristics
HA01(HA02)	Δ*AcsA*::$P_{cLac143}$-*pmHAS(-sfGFP)*	HA producing, without or with sfGFP
HA03(HA04)	Δ*AcsA*::$P_{cLac143}$-*seHasA(-sfGFP)*	HA producing, without or with sfGFP
HA06	Δ*glgA2*::Km^R +Δ*AcsA*::$P_{cLac143}$-*pmHAS*	Partial glycogen depletion, HA producing
HA07	Δ*glgA1*::Cm^R +Δ*AcsA*::$P_{cLac143}$-*pmHAS*	Partial glycogen depletion, HA producing
HA08	Δ*cesA*::Cm^R +Δ*AcsA*::$P_{cLac143}$-*pmHAS*	Cellulose depletion, HA producing
HA11	Δ*glpK*::P_{cpt}-*glmS-glmU*-Cm^R +Δ*AcsA*::$P_{cLac143}$-*pmHAS*	Overexpression of heterologous UDP-GlcNAc pathway enzymes, HA producing
HA12	Δ*glgA1*::P_{cpt}-*glmS-glmU*-Cm^R +Δ*AcsA*::$P_{cLac143}$-*pmHAS*	Overexpression of heterologous UDP-GlcNAc pathway enzymes, partial glycogen depletion, HA producing
HA13	Δ*glgA2*::P_{cpc560}-*tuaD-gtaB*-Km^R +Δ*AcsA*::$P_{cLac143}$-*pmHAS*	Overexpression of heterologous UDP-GlcUA pathway enzymes, partial glycogen depletion, HA producing

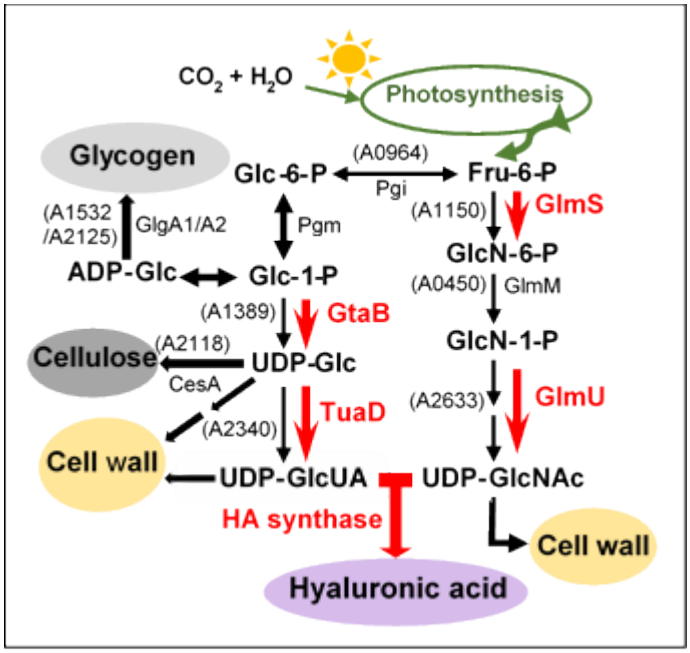

Figure 1. Schematic pathway for hyaluronic acid precursor biosynthesis in Syn7002 (adapted from [16]). Red arrows indicate heterologous enzymes commonly used to strengthen the precursors biosynthesis and HA formation in heterotrophic bacteria; equivalent, functionally proven or predicted enzymes from Syn7002 are shown in brackets. Selected potential competing pathway, such as glycogen, cellulose or cell wall biosynthesis are also marked with coloured-in circles. Glc-6-P: glucose-6-phosphate; Glc-1-P: glucose-1-phosphate; ADP-Glc: ADP-glucose; UDP-Glc: UDP-glucose; UDP-GlcUA: UDP-glucuronic acid; Fru-6-P: fructose-6-phosphate; GlcN-6-P: glucosamine-6-phosphate; GlcN-1-P: glucosamine-1-phosphate; GlcNAc-1-P: N-acetylglucosamine-1-phosphate; UDP-GlcNAc: UDP-N-acetylglucosamine; TuaD: UDP-glucose dehydrogenase; GtaB: UDP-glucose pyrophosphorylase; GlmS: glutamine amidotransferase; GlmU: acetyl-CoA acetyltransferase/pyrophosphorylase; GlgA1/A2: glycogen synthase A1/A2; CesA: cellulose synthase; Pgi: phosphoglucoseisomerase; Pgm: phosphoglucomutase

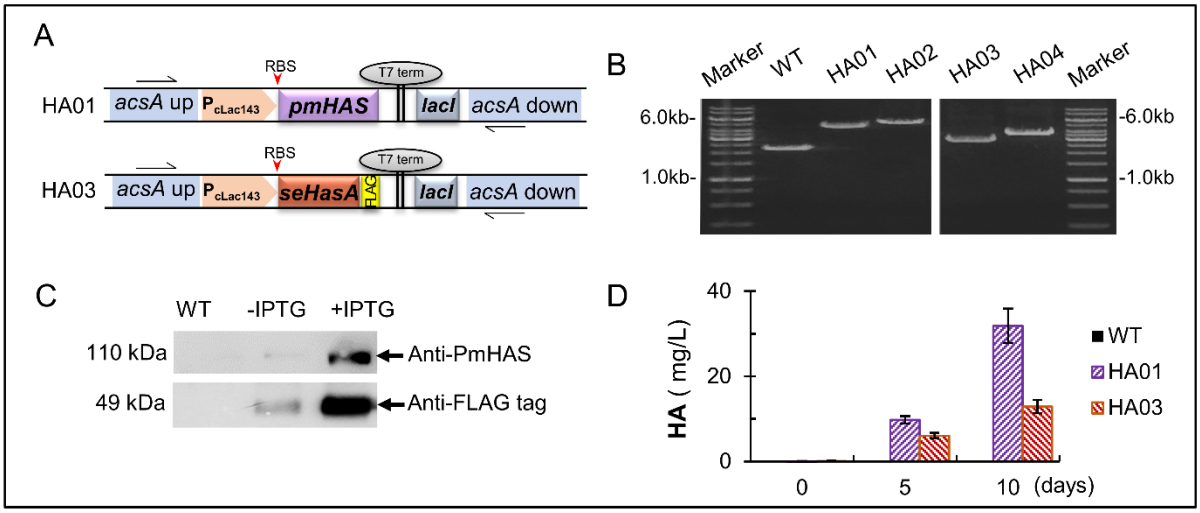

Figure 2. Introduction of two different HA synthases into Syn7002. **A.** Artificial operons used for expression of different HA synthases from the *acsA* locus of Syn7002, controlled by the inducible promoter $P_{cLac143}$. **B.** Genomic DNA PCR analysis of strains with *pmHAS* (HA01) or *seHasA* (HA03), as well as their *sfGFP*-tagged version (HA02 and HA04), with specific primers listed in Table S1. Expected PCR sizes are 4773 bp for strain HA01, 5508 bp for strain HA02, 3279 bp for HA03, 3983 bp for HA04 and 2303 bp for the *acsA* WT locus. **C.** Western blot analysis of PmHAS or SeHasA expression in response to IPTG addition, using either anti-PmHAS or anti-FLAG antibodies, respectively. **D.** Quantification of HA in the growth medium in cultures induced with 1mM IPTG, at the time points indicated. Error bars represent standard deviation of three biological replicates (n=3), measured in duplicate. HA01: Δ*acsA*::$P_{cLac143}$-*pmHAS*; HA02: Δ*acsA*::$P_{cLac143}$-*pmHAS-sfGFP*; HA03: Δ*acsA*::$P_{cLac143}$-*seHasA*; HA04: Δ*acsA*::$P_{cLac143}$-*seHasA-sfGFP*.

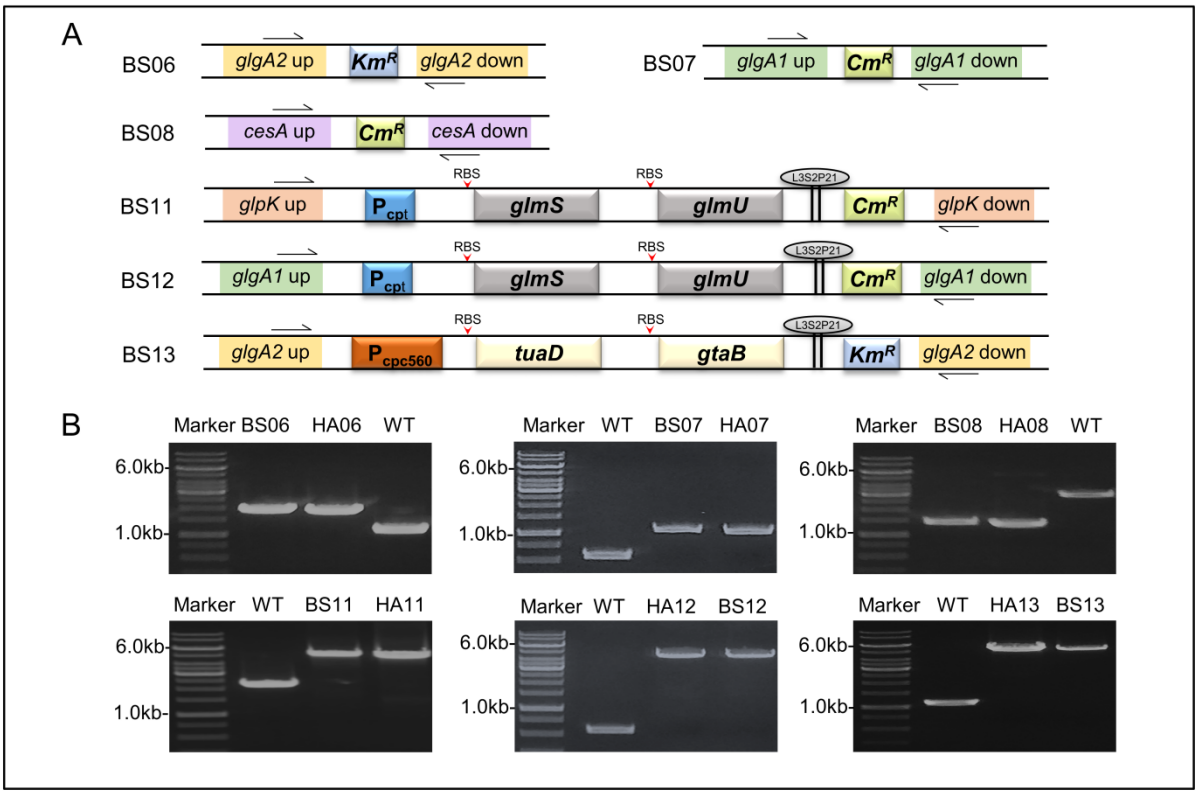

Figure 3. Overview of the different modifications for improved PmHAS-dependent HA production in Syn7002. **A.** Schematic images of constructs used for deletion of competing pathways and heterologous expression of precursor biosynthesis artificial operons. **B.** Gel images of gDNA PCR segregation tests for all background strains (BS##) and their corresponding PmHAS containing strains (HA##) constructed in this work. Primers used for segregation testing are listed in Table S1. Expected PCR product sizes are: 1470bp (BS06 and HA06), 1108bp (BS07 and HA07), 1365bp (BS08 and HA08), 4723bp (BS11 and HA11), 4955bp (BS12 and HA12) and 4199bp (BS13 and HA13). The corresponding expected PCR sizes in WT are 576bp (*glgA1*), 938bp (*glgA2*), 2097bp (*glpK*) and 2863bp (*cesA*). HA06: Δ*glgA2*::*Km*^{R} +Δ*acsA*::P$_{cLac143}$-*pmHAS*; HA07: Δ*glgA1*::*Cm*^{R} +Δ*acsA*::P$_{cLac143}$-*pmHAS*; HA08: Δ*cesA*::*Cm*^{R} +Δ*acsA*::P$_{cLac143}$-*pmHAS*; HA11: *glpK*::P$_{cpt}$-*glmS-glmU-Cm*^{R}+Δ*acsA*::P$_{cLac143}$-*pmHAS*; HA12: Δ*glgA1*::P$_{cpt}$-*glmS-glmU-Cm*^{R}+Δ*acsA*::P$_{cLac143}$-*pmHAS*; HA13: Δ*glgA2*::P$_{cpc560}$-*tuaD-gtaB-Km*^{R}+Δ*acsA*::P$_{cLac143}$-*pmHAS*

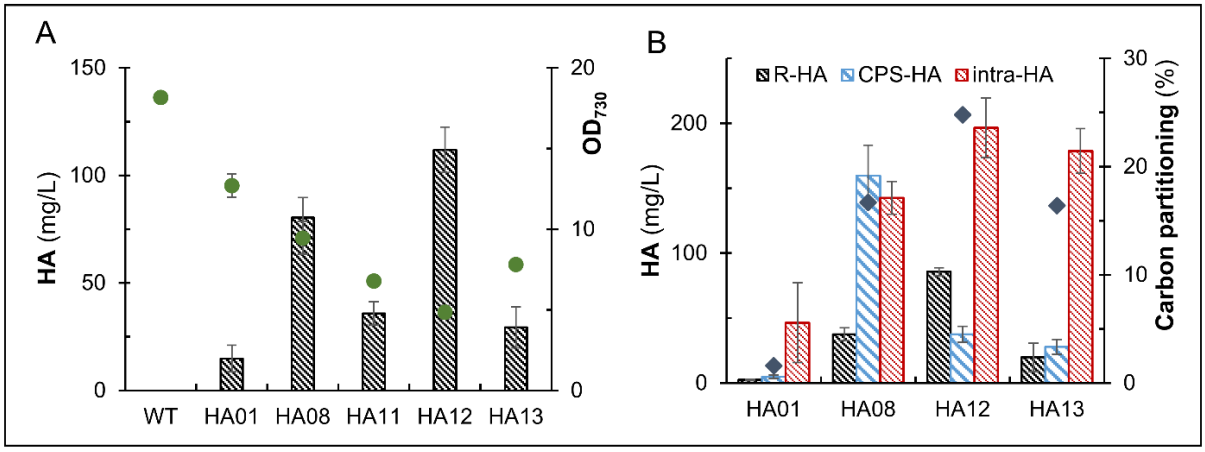

Figure 4. HA production by different strains. **A.** HA production (bar graphs) and cell density (dot plots) comparison at 5 days post IPTG induction. **B.** Assessment of HA quantification in different fractions, as well as the calculated photosynthethic carbon partitioning to total HA production (diamond plots). R-HA: HA released into growth medium; CPS-HA: capsular HA attached to cell surface; intra-HA: intracellular HA. Error bars represent standard deviation of technical triplicates. HA01: Δ*acsA*::$P_{cLac143}$-*pmHAS*; HA08: Δ*cesA*::Cm^R +Δ*acsA*::$P_{cLac143}$-*pmHAS*; HA11: *glpK*::P_{cpt}-*glmS-glmU-*Cm^R+Δ*acsA*::$P_{cLac143}$-*pmHAS*; HA12: Δ*glgA1*::P_{cpt}-*glmS-glmU-*Cm^R+Δ*acsA*::$P_{cLac143}$-*pmHAS*; HA13: Δ*glgA2*::P_{cpc560}-*tuaD-gtaB-*Km^R+Δ*acsA*::$P_{cLac143}$-*pmHAS*.

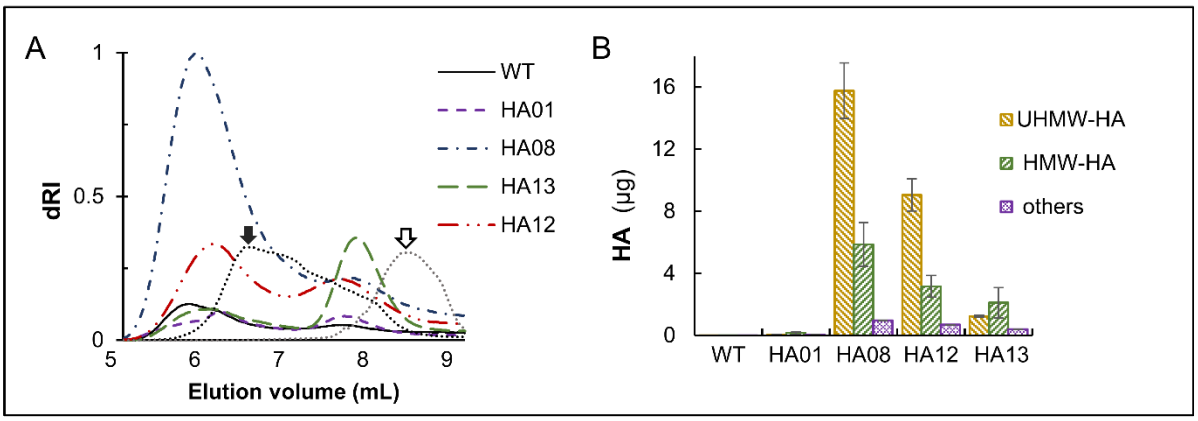

Figure 5. Size estimation of HA polymers from different strain by HPLC-SEC. **A.** Chromatograms of released polymers from different HA producing strains. Black filled arrow: commercial HA (molecular mass 2-2.2MDa); black outlined arrow: PEG polymer standard (molecular mass 1 MDa). **B.** HA content in each eluted peak. Peaks were eluted according to the intensity changes of dRI detector (elution times may vary between samples of different HA producing strains). Error bars represent standard deviation of technical duplicates. HA01: Δ*acsA*::$P_{cLac143}$-*pmHAS*; HA08: Δ*cesA*::Cm^R +Δ*acsA*::$P_{cLac143}$-*pmHAS*; HA12: Δ*glgA1*::P_{cpt}-*glmS-glmU-*Cm^R+Δ*acsA*::$P_{cLac143}$-*pmHAS*; HA13: Δ*glgA2*::P_{cpc560}-*tuaD-gtaB-*Km^R+Δ*acsA*::$P_{cLac143}$-*pmHAS*.

Supplementary materials

Table S1. List of primers used in this work.

Table S2. List of plasmids constructed in this work.

Table S3. Estimation of total fixed carbon partitioning to HA in different producing strains.

Figure S1. Introduction and expression of two different HA synthases into Syn7002.

Figure S2. Confocal microscopy images of Syn7002 cells expressing HA synthase.

Figure S3. Hyaluronidase digestion of cyanobacterial HA compared to commercial HA.

Figure S4. LC-MS/MS analysis of hyaluronidase digested samples from strain HA01 and commercial HA.

Figure S5. Effect of partial glycogen depletion on growth and HA production in Syn7002 strains, at 5 days post-IPTG induction.

Figure S6. FTIR spectra of commercial HA and HPLC-purified HA produced by different strains.

5. References

[1] H. Niederholtmeyer, B.T. Wolfstadter, D.F. Savage, P.A. Silver, J.C. Way, Engineering cyanobacteria to synthesize and export hydrophilic products, Appl Environ Microb, 76 (2010) 3462-3466.

[2] C.J. Knoot, J. Ungerer, P.P. Wangikar, H.B. Pakrasi, Cyanobacteria: Promising biocatalysts for sustainable chemical production, J Biol Chem, 293 (2018) 5044-5052.

[3] G.D. Luan, X.F. Lu, Tailoring cyanobacterial cell factory for improved industrial properties, Biotechnol Adv, 36 (2018) 430-442.

[4] D.C. Ducat, J.C. Way, P.A. Silver, Engineering cyanobacteria to generate high-value products, Trends Biotechnol, 29 (2011) 95-103.

[5] A. Sarnaik, M.H. Abernathy, X.R. Han, Y.L. Ouyang, K. Xia, Y. Chen, B. Cress, F.M. Zhang, A. Lali, R. Pandit, R.J. Linhardt, Y.J. Tang, M.A.G. Koffas, Metabolic engineering of cyanobacteria for photoautotrophic production of heparosan, a pharmaceutical precursor of heparin, Algal Res, 37 (2019) 57-63.

[6] C.G. Boeriu, J. Springer, F.K. Kooy, L.A.M. van den Broek, G. Eggink, Production methods for hyaluronan, International Journal of Carbohydrate Chemistry, 2013 (2013) 1-14.

[7] N. Volpi, J. Schiller, R. Stern, L. Soltes, Role, metabolism, chemical modifications and applications of hyaluronan, Curr Med Chem, 16 (2009) 1718-1745.

[8] Hyaluronic Acid Market Size Worth USD 15.4 Billion by 2025, Grand View Research.

[9] L. Liu, Y.F. Liu, J.H. Li, G.C. Du, J. Chen, Microbial production of hyaluronic acid: current state, challenges, and perspectives, Microb Cell Fact, 10 (2011) 99-107.

[10] A. Zakeri, M.J. Rasaee, N. Pourzardosht, Enhanced hyluronic acid production in Streptococcus zooepidemicus by over expressing HasA and molecular weight control with Niscin and glucose, Biotechnol Rep (Amst), 16 (2017) 65-70.

[11] J.-H. Kim, S.-J. Yoo, D.-K. Oh, Y.-G. Kweon, D.-W. Park, C.-H. Lee, G.-H. Gil, Selection of a *Streptococcus equi* mutant and optimization of culture conditions for the production of high molecular weight hyaluronic acid, Enzyme and Microbial Technology, 19 (1996) 440-445.

[12] H.M. Yu, G. Stephanopoulos, Metabolic engineering of *Escherichia coli* for biosynthesis of hyaluronic acid, Metab Eng, 10 (2008) 24-32.

[13] Z.C. Mao, H.D. Shin, R. Chen, A recombinant *E. coli* bioprocess for hyaluronan synthesis, Appl Microbiol Biot, 84 (2009) 63-69.

[14] Y.N. Jia, J. Zhu, X.F. Chen, D.Y. Tang, D. Su, W.B. Yao, X.D. Gao, Metabolic engineering of *Bacillus subtilis* for the efficient biosynthesis of uniform hyaluronic acid with controlled molecular weights, Bioresource Technol, 132 (2013) 427-431.

[15] P. Jin, Z. Kang, P.H. Yuan, G.C. Du, J. Chen, Production of specific-molecular-weight hyaluronan by metabolically engineered *Bacillus subtilis* 168, Metab Eng, 35 (2016) 21-30.

[16] B. Widner, R. Behr, S. Von Dollen, M. Tang, T. Heu, A. Sloma, D. Sternberg, P.L. DeAngelis, P.H. Weigel, S. Brown, Hyaluronic acid production in *Bacillus subtilis*, Appl Environ Microb, 71 (2005) 3747-3752.

[17] Z.C. Mao, R.R. Chen, Recombinant synthesis of hyaluronan by *Agrobacterium sp.*, Biotechnol Progr, 23 (2007) 1038-1042.

[18] M.H. Abernathy, J. Yu, F. Ma, M. Liberton, J. Ungerer, W.D. Hollinshead, S. Gopalakrishnan, L. He, C.D. Maranas, H.B. Pakrasi, D.K. Allen, Y.J. Tang, Deciphering

cyanobacterial phenotypes for fast photoautotrophic growth via isotopically nonstationary metabolic flux analysis, Biotechnol Biofuels, 10 (2017) 273-285.

[19] B.W. Abramson, J. Lensmire, Y.T. Lin, E. Jennings, D.C. Ducat, Redirecting carbon to bioproduction via a growth arrest switch in a sucrose-secreting cyanobacterium, Algal Res, 33 (2018) 248-255.

[20] C. Zhao, Z.K. Li, T. Li, Y.J. Zhang, D.A. Bryant, J.D. Zhao, High-yield production of extracellular type-I cellulose by the cyanobacterium *Synechococcus* sp PCC 7002, Cell Discov, 1 (2015) 15004-15015.

[21] P. Flombaum, J.L. Gallegos, R.A. Gordillo, J. Rincon, L.L. Zabala, N. Jiao, D.M. Karl, W.K. Li, M.W. Lomas, D. Veneziano, C.S. Vera, J.A. Vrugt, A.C. Martiny, Present and future global distributions of the marine Cyanobacteria Prochlorococcus and Synechococcus, Proc Natl Acad Sci U S A, 110 (2013) 9824-9829.

[22] D.S. Snyder, B. Brahamsha, P. Azadi, B. Palenik, Structure of compositionally simple lipopolysaccharide from marine synechococcus, J Bacteriol, 191 (2009) 5499-5509.

[23] I. Stewart, P.J. Schluter, G.R. Shaw, Cyanobacterial lipopolysaccharides and human health - a review, Environ Health, 5 (2006) 7-29.

[24] M. Klemenčič, A.Z. Nielsen, Y. Sakuragi, N.U. Frigaard, H. Čelešnik, P.E. Jensen, D. M., Synthetic biology of cyanobacteria for production of biofuels and high-value products, in: C. Gonzalez-Fernandez, R. Muñoz (Eds.), Microalgae-Based Biofuels and Bioproducts, Woodhead Publishing, 2017, pp. 305-325.

[25] T.T. Selao, A. Wlodarczyk, P.J. Nixon, B. Norling, Growth and selection of the cyanobacterium *Synechococcus sp.* PCC 7002 using alternative nitrogen and phosphorus sources, Metab Eng, 54 (2019) 255-263.

[26] M.B. Begemann, E.K. Zess, E.M. Walters, E.F. Schmitt, A.L. Markley, B.F. Pfleger, An organic acid based counter selection system for cyanobacteria, Plos One, 8 (2013) 76594-76605.

[27] J. Zhou, H.F. Zhang, H.K. Meng, Y. Zhu, G.H. Bao, Y.P. Zhang, Y. Li, Y.H. Ma, Discovery of a super-strong promoter enables efficient production of heterologous proteins in cyanobacteria, Sci Rep-Uk, 4 (2014) 4500-4505.

[28] A.L. Markley, M.B. Begemann, R.E. Clarke, G.C. Gordon, B.F. Pfleger, Synthetic biology toolbox for controlling gene expression in the cyanobacterium *Synechococcus* sp. strain PCC 7002, Acs Synth Biol, 4 (2015) 595-603.

[29] M. Kostylev, A.E. Otwell, R.E. Richardson, Y. Suzuki, Cloning should be smple: *Escherichia coli* DH5 alpha-mediated assembly of multiple DNA fragments with short end fomologies, Plos One, 10 (2015) 1371-1385.

[30] A.M. Ruffing, Improved Free Fatty Acid Production in Cyanobacteria with *Synechococcus sp. PCC 7002* as Host, Frontiers in bioengineering and biotechnology, 2 (2014) 17-26.

[31] L.N. Liu, S.J. Bryan, F. Huang, J.F. Yu, P.J. Nixon, P.R. Rich, C.W. Mullineaux, Control of electron transport routes through redox-regulated redistribution of respiratory complexes, P Natl Acad Sci USA, 109 (2012) 11431-11436.

[32] T.T. Selao, L.F. Zhang, J. Knoppova, J. Komenda, B. Norling, Photosystem II assembly steps take place in the thylakoid membrane of the cyanobacterium *Synechocystis sp* PCC6803, Plant Cell Physiol, 57 (2016) 95-104.

[33] T.M.M. Bernaerts, L. Gheysen, C. Kyomugasho, Z.J. Kermani, S. Vandionant, I. Foubert, M.E. Hendrickx, A.M. Van Loey, Comparison of microalgal biomasses as functional food ingredients: Focus on the composition of cell wall related polysaccharides, Algal Res, 32 (2018) 150-161.

[34] R. Dephilippis, M.C. Margheri, E. Pelosi, S. Ventura, Exopolysaccharide Production by a Unicellular Cyanobacterium Isolated from a Hypersaline Habitat, J Appl Phycol, 5 (1993) 387-394.

[35] Z.Q. Zhang, J. Xie, J. Liu, R.J. Linhardt, Tandem MS can distinguish hyaluronic acid from N-acetylheparosan, J Am Soc Mass Spectr, 19 (2008) 82-90.

[36] A.V. Kuhn, K. Raith, V. Sauerland, R.H.H. Neubert, Quantification of hyaluronic acid fragments in pharmaceutical formulations using LC-ESI-MS, J Pharmaceut Biomed, 30 (2003) 1531-1537.

[37] S. Haserodt, M. Aytekin, R.A. Dweik, A comparison of the sensitivity, specificity, and molecular weight accuracy of three different commercially available Hyaluronan ELISA-like assays, Glycobiology, 21 (2011) 175-183.

[38] S.G. Ball, M.K. Morell, From bacterial glycogen to starch: understanding the biogenesis of the plant starch granule, Annu Rev Plant Biol, 54 (2003) 207-233.

[39] M.L. Fisher, R. Allen, Y.Q. Luo, R. Curtiss, Export of extracellular polysaccharides modulates adherence of the cyanobacterium *Synechocystis*, Plos One, 8 (2013) 74514-74523.

[40] Y. Xu, L.T. Guerra, Z.K. Li, M. Ludwig, G.C. Dismukes, D.A. Bryant, Altered carbohydrate metabolism in glycogen synthase mutants of *Synechococcus* sp strain PCC 7002: Cell factories for soluble sugars, Metab Eng, 16 (2013) 56-67.

[41] J.D. de Oliveira, L.S. Carvalho, A.M.V. Gomes, L.R. Queiroz, B.S. Magalhaes, N.S. Parachin, Genetic basis for hyper production of hyaluronic acid in natural and engineered microorganisms, Microb Cell Fact, 15 (2016) 119-137.

[42] J.W. Chwa, W.J. Kim, S.J. Sim, Y. Um, H.M. Woo, Engineering of a modular and synthetic phosphoketolase pathway for photosynthetic production of acetone from CO_2 in *Synechococcus elongatus* PCC 7942 under light and aerobic condition, Plant Biotechnol J, 14 (2016) 1768-1776.

[43] A.J. De Porcellinis, H. Norgaard, L.M.F. Brey, S.M. Erstad, P.R. Jones, J.L. Heazlewood, Y. Sakuragi, Overexpression of bifunctional fructose-1,6-bisphosphatase/sedoheptulose-1,7-bisphosphatase leads to enhanced photosynthesis and global reprogramming of carbon metabolism in *Synechococcus sp* PCC 7002, Metab Eng, 47 (2018) 170-183.

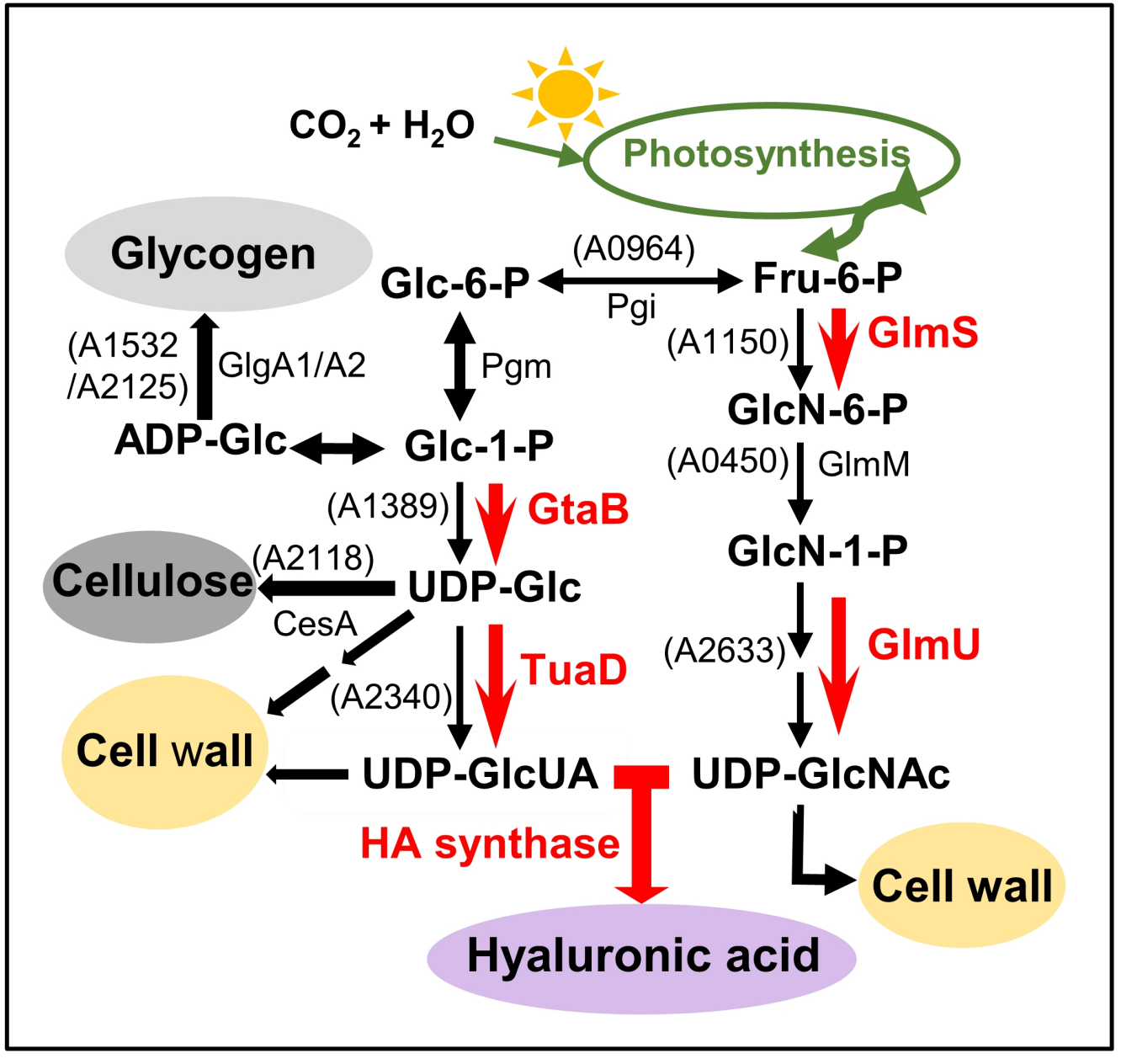
$CO_2 + H_2O$
Photosynthesis
Glycogen
(A0964)
Glc-6-P
Pgi
Fru-6-P
(A1532
/A2125)
GlgA1/A2
Pgm
(A1150)
GlmS
GlcN-6-P
ADP-Glc
Glc-1-P
(A0450)
GlmM
(A1389)
GtaB
GlcN-1-P
Cellulose
(A2118)
UDP-Glc
CesA
(A2633)
GlmU
TuaD
(A2340)
Cell wall
UDP-GlcUA
UDP-GlcNAc
HA synthase
Cell wall
Hyaluronic acid

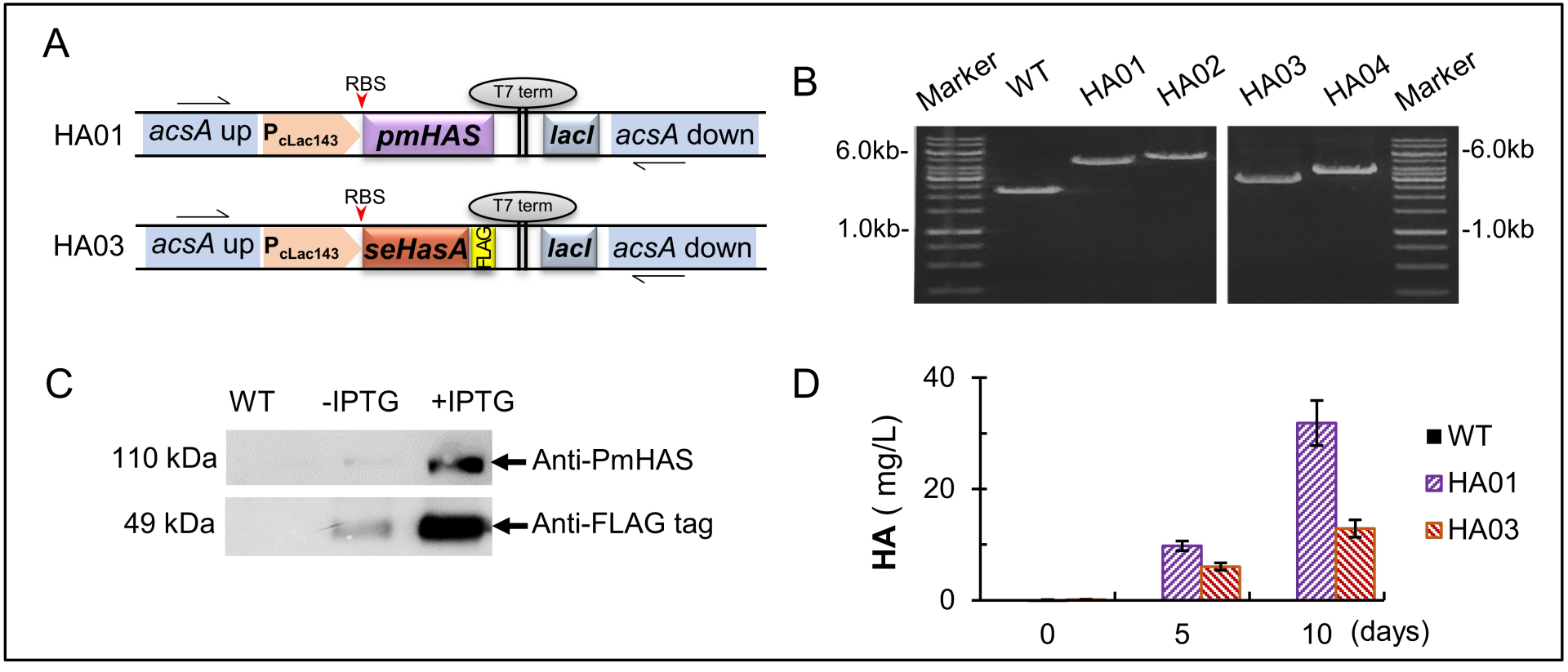
A
RBS
T7 term
HA01
acsA up
P cLac143
pmHAS
lacI
acsA down
RBS
T7 term
HA03
acsA up
P cLac143
seHasA
FLAG
lacI
acsA down
B
Marker
WT
HA01
HA02
HA03
HA04
Marker
6.0kb-
1.0kb-
-6.0kb
-1.0kb
C
WT
-IPTG
+IPTG
110 kDa
Anti-PmHAS
49 kDa
Anti-FLAG tag
D
HA (mg/L)
40
20
0
0
5
10
(days)
WT
HA01
HA03

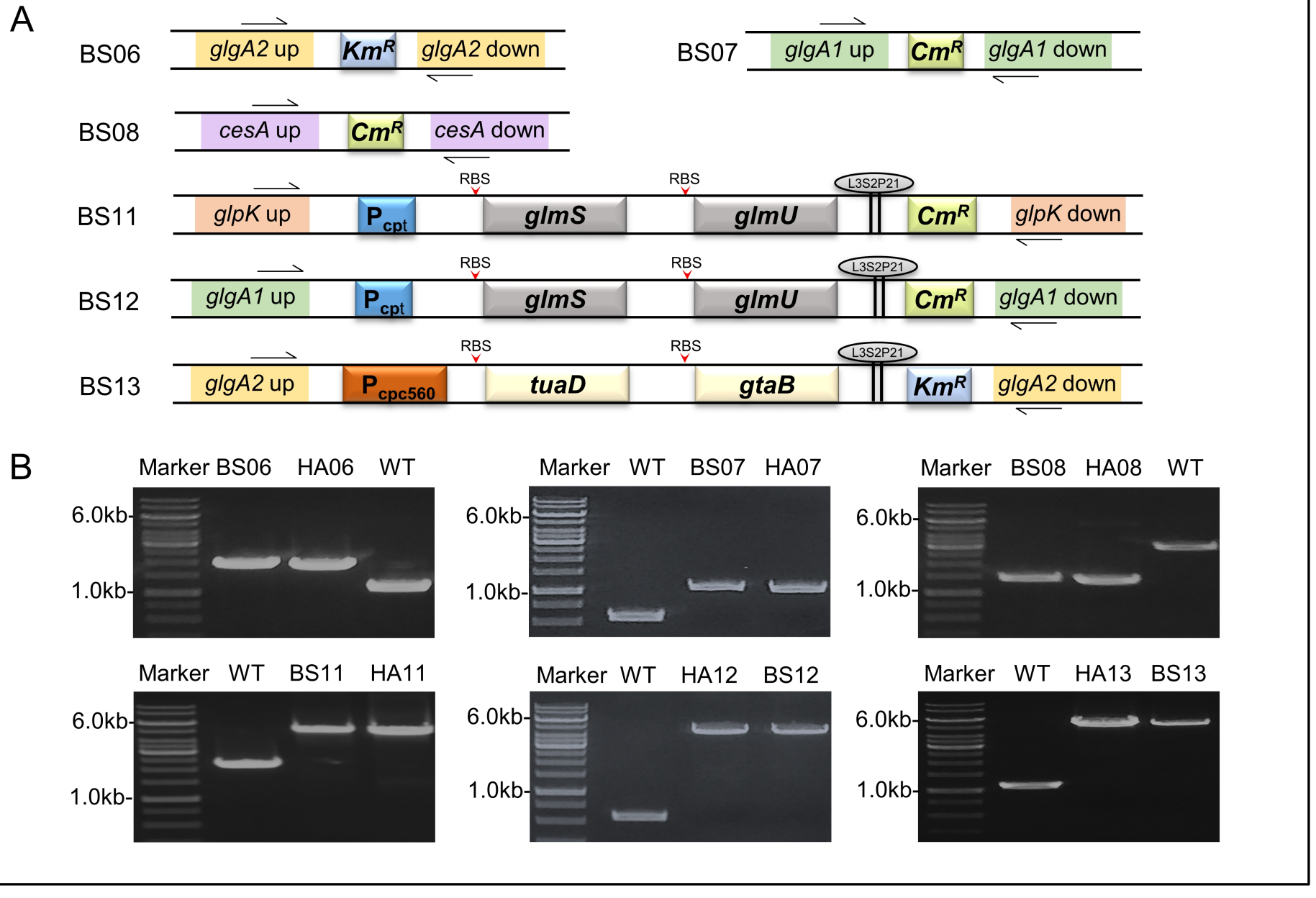
A
BS06
glgA2 up
Km^R
glgA2 down
BS07
glgA1 up
Cm^R
glgA1 down
BS08
cesA up
Cm^R
cesA down
BS11
glpK up
P cpt
RBS
glmS
RBS
glmU
L3S2P21
Cm^R
glpK down
BS12
glgA1 up
P cpt
RBS
glmS
RBS
glmU
L3S2P21
Cm^R
glgA1 down
BS13
glgA2 up
P cpc560
RBS
tuaD
RBS
gtaB
L3S2P21
Km^R
glgA2 down
B
Marker BS06 HA06 WT
6.0kb
1.0kb
Marker WT BS07 HA07
6.0kb
1.0kb
Marker BS08 HA08 WT
6.0kb
1.0kb
Marker WT BS11 HA11
6.0kb
1.0kb
Marker WT HA12 BS12
6.0kb
1.0kb
Marker WT HA13 BS13
6.0kb
1.0kb

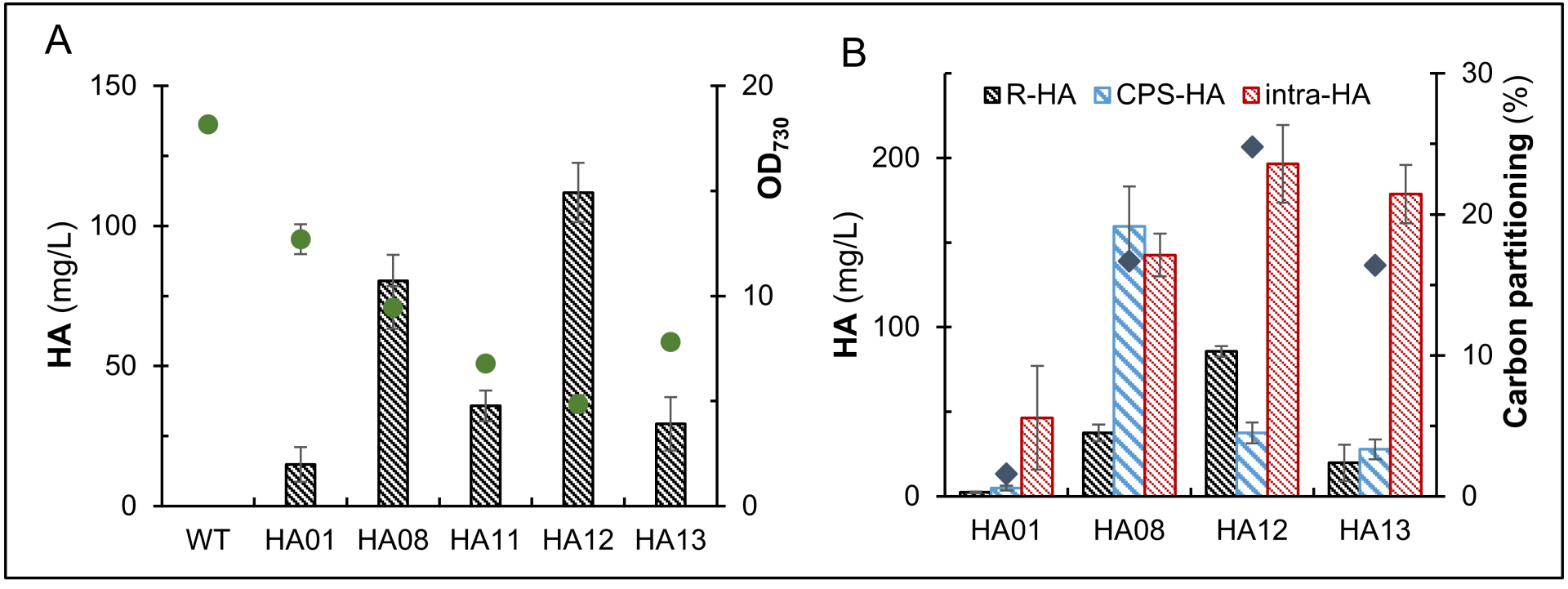
A
150
100
50
0
HA (mg/L)
20
10
0
OD730
WT
HA01
HA08
HA11
HA12
HA13
B
R-HA
CPS-HA
intra-HA
200
100
0
HA (mg/L)
30
20
10
0
Carbon partitioning (%)
HA01
HA08
HA12
HA13

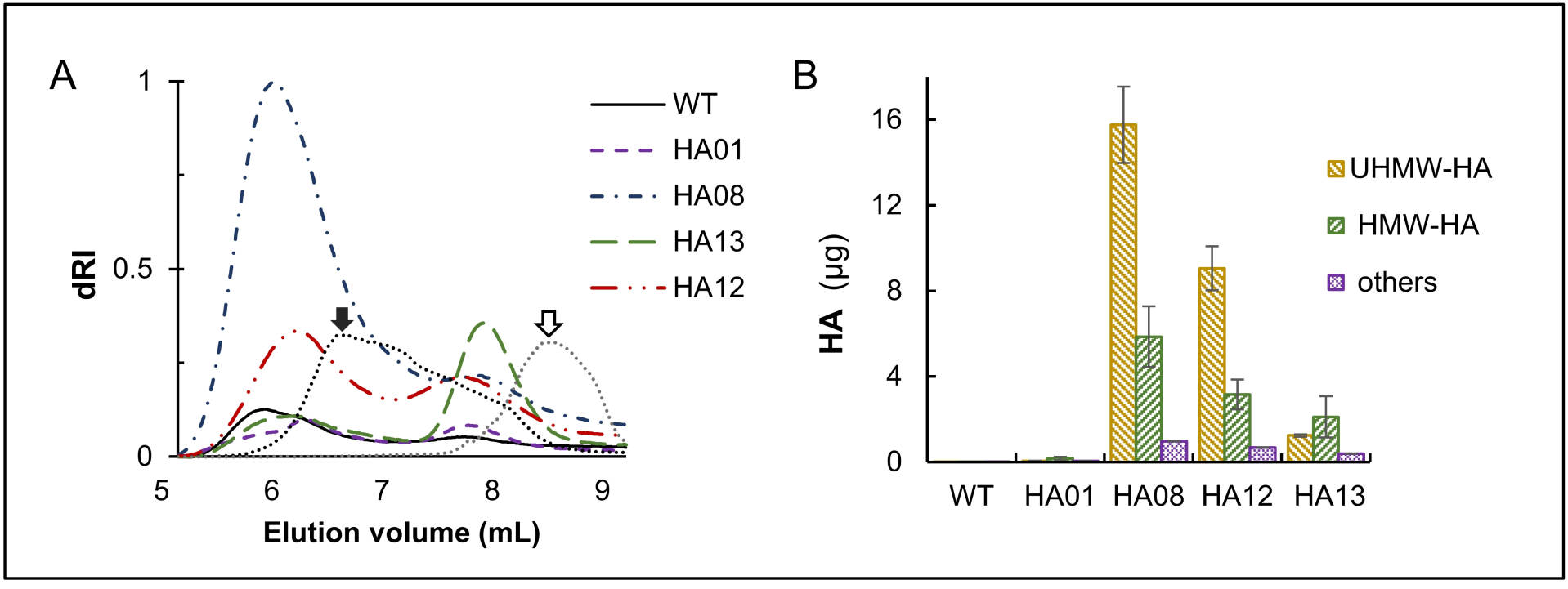
A
1
0.5
0
dRI
5
6
7
8
9
Elution volume (mL)
WT
HA01
HA08
HA13
HA12
B
16
12
8
4
0
HA (μg)
UHMW-HA
HMW-HA
others
WT
HA01
HA08
HA12
HA13

Conflict of Interest Declaration

We wish to confirm that there are no known conflicts of interest associated with this publication and there has been no significant financial support for this work that could have influenced its outcome.

We confirm that the manuscript has been read and approved by all named authors and that there are no other persons who satisfied the criteria for authorship but are not listed. We further confirm that the order of authors listed in the manuscript has been approved by all of us.

We confirm that we have given due consideration to the protection of intellectual property associated with this work and that there are no impediments to publication, including the timing of publication, with respect to intellectual property. In so doing we confirm that we have followed the regulations of our institutions concerning intellectual property.

We understand that the Corresponding Author is the sole contact for the Editorial process (including Editorial Manager and direct communications with the office). She is responsible for communicating with the other authors about progress, submissions of revisions and final approval of proofs. We confirm that we have provided a current, correct email address which is accessible by the Corresponding Author.

Signed by all authors as follows, on the 31st May 2019:

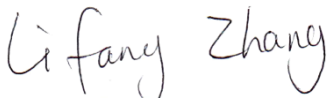 Lifang Zhang	 Peter J. Nixon
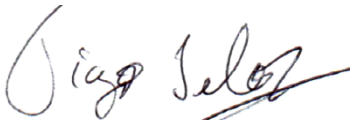 Tiago Selão	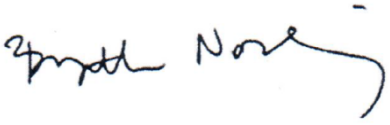 Birgitta Norling

Supplementary material

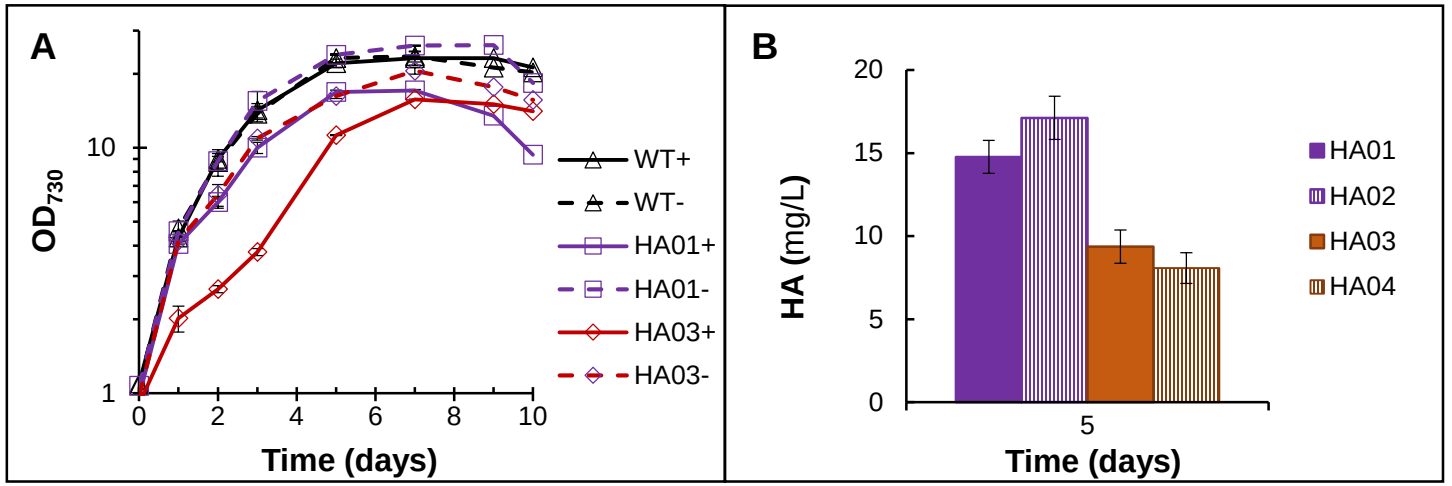

Figure S1. The effects of two different HA synthases on growth and HA production in Syn7002 strains. **A**. Growth curve of strains expressing HA synthases with (+) or without (-) 1mM IPTG. **B.** HA quantification in the growth medium 5 days post IPTG induction. Error bars represent standard deviation of biological duplicate measured in duplicate. HA01: Δ*acsA*::*PcLac143-pmHAS*; HA02: Δ*acsA*::*PcLac143-pmHAS-sfGFP*; HA03: Δ*acsA*::*PcLac143-seHasA*; HA04: Δ*acsA*::*PcLac143-seHasA-sfGFP*.

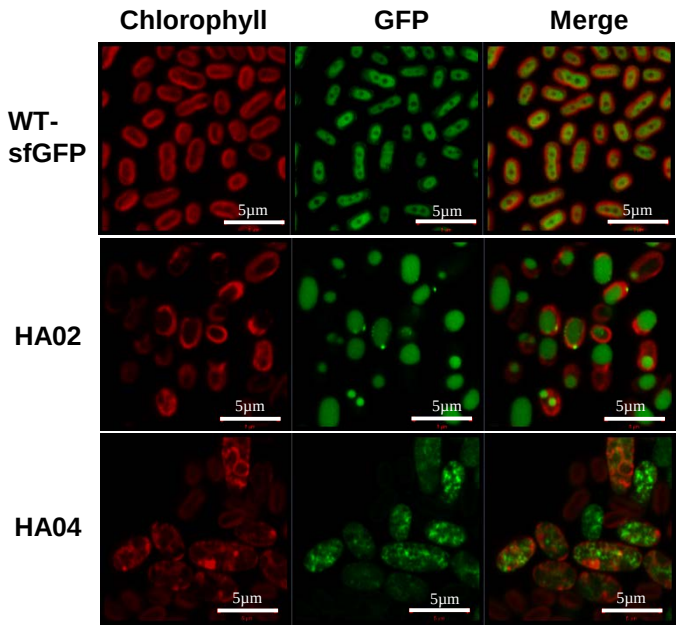

Figure S2. Confocal microscopy images of Syn7002 cells expressing different HA synthases. Two days post IPTG induction cultures of WT-sfGFP, HA02 (expressing PmHAS-sfGFP) and HA04 (expressing SeHasA-sfGFP) were used for imaging. Scale bar (in white): 5µm. HA02: Δ*acsA*::$P_{cLac143}$-*pmHAS-sfGFP*; HA04: Δ*acsA*::$P_{cLac143}$-*seHasA-sfGFP*.

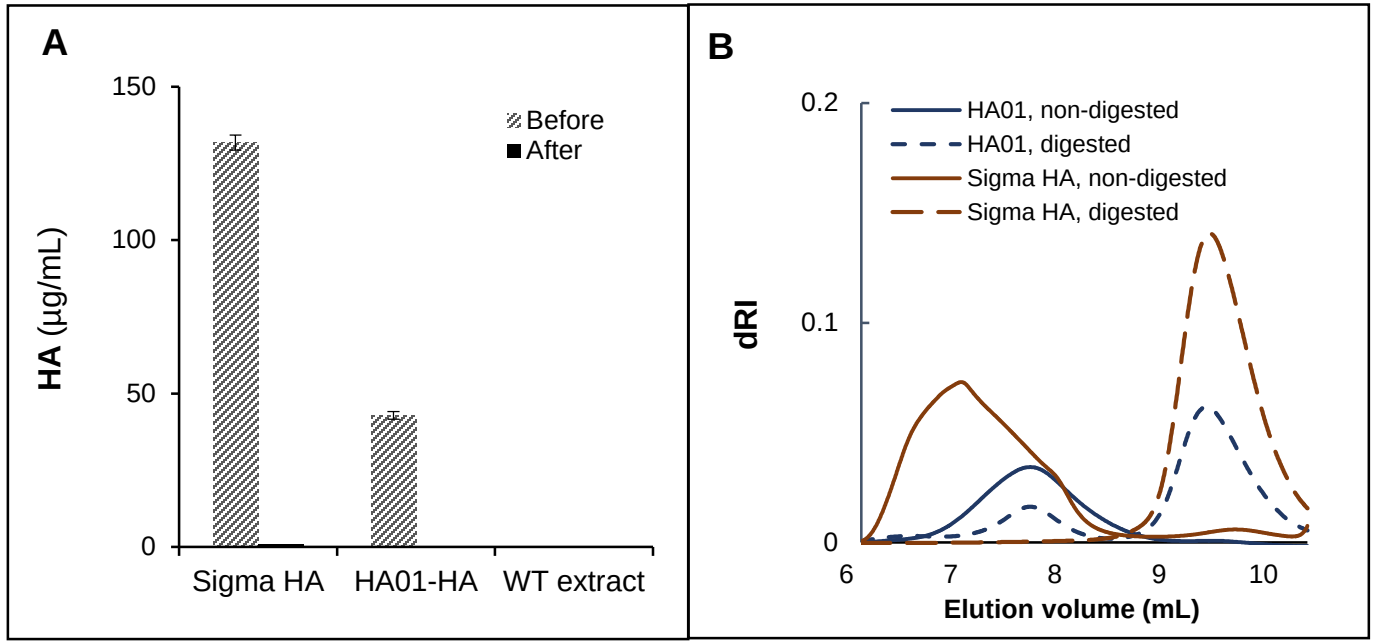

Figure S3. Hyaluronidase digestion of cyanobacterial HA compared to commercial HA. **A.** Quantification of commercial HA (purchased from Sigma), samples extracted from strain HA01 (HA01-HA) and Syn7002 WT before and after hyaluronidase digestion. Error bars represent standard deviation of technical triplicates. **B.** Chromatograms of hyaluronidase digested vs non-digested extract from strain HA01 and Sigma HA.

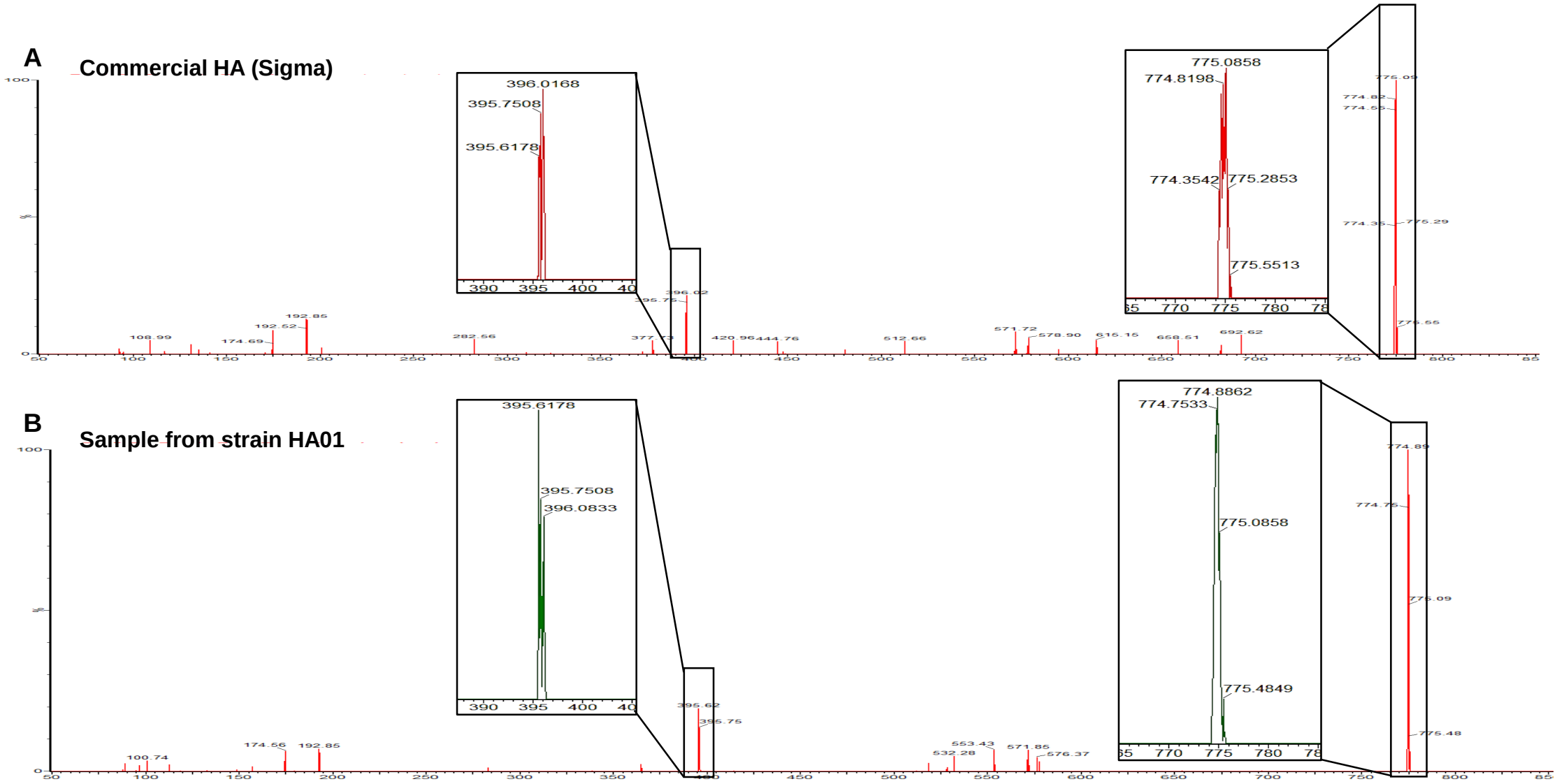

Figure S4. LC-MS/MS analysis of hyaluronidase digested samples from strain HA01 and commercial HA. **A.** Digested commercial HA from Sigma; **B.** Digested cyanobacterial HA produced by strain HA01. Insets are enlarged versions of the m/z spectra regions containing typical peaks of HA disaccharides (≈395.7) and tetrasaccharides (≈774.9).

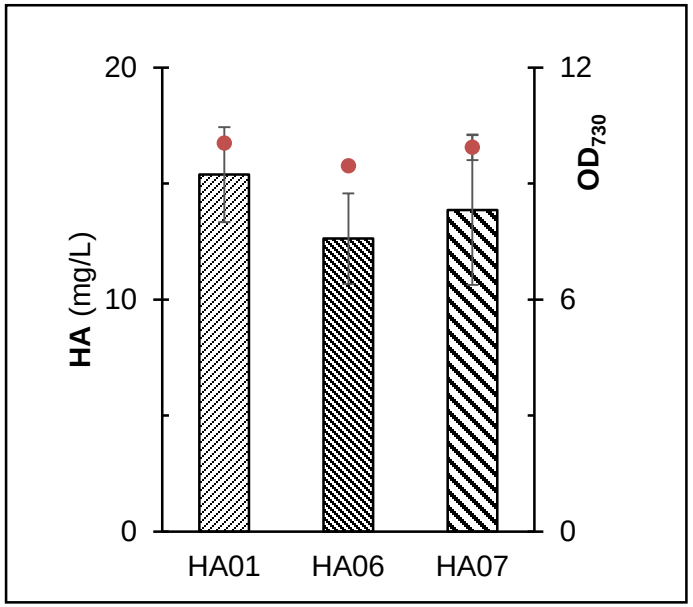

Figure S5. Effect of partial glycogen depletion on growth (dot plots) and HA production (bar graphs) in Syn7002 strains, at 5 days post-IPTG induction. Error bars represent standard deviation of biological duplicates measured in duplicate. HA01: Δ*acsA*::$P_{cLac143}$-*pmHAS*; HA06: Δ*glgA2*::Km^R+Δ*acsA*::$P_{cLac143}$-*pmHAS*; HA07: Δ*glgA1*::Cm^R+Δ*acsA*::$P_{cLac143}$-*pmHAS* .

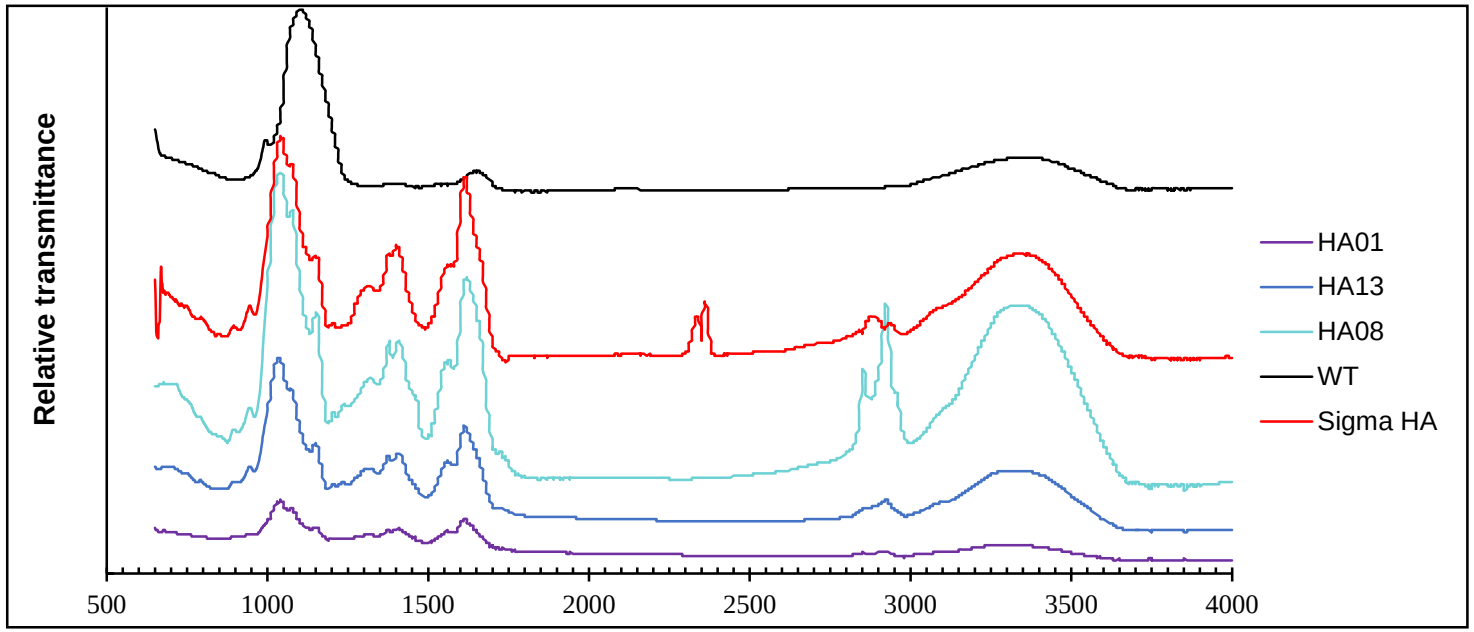

Figure S6. FTIR spectra of commercial HA and HPLC-purified HA produced by different strains (UHMW-HA peak from strain HA08, HMW-HA from strains HA01 and HA13, see Figure ~~65~~a). All the Syn7002-produced HA and commercial HA showed typical peaks at 1043.3 cm^{-1} due to the C-O-C stretching, at 1411.64 cm^{-1} corresponding to C-O groups in combination with C=O, at 1616.06 cm^{-1}, indicative of amide II groups, at 2892.7 cm^{-1} due to C-H stretching and at 3407.6 cm^{-1}, attributable to OH stretching. The small peaks observed for Sigma HA at 2350 and 2370 cm^{-1} are due to residual CO_2 in the system. HA01: Δ*acsA*::$P_{cLac143}$-*pmHAS*; HA08: Δ*cesA*::Cm^R+Δ*acsA*::$P_{cLac143}$-*pmHAS*; HA13: Δ*glgA2*::P_{cpc560}-*tuaD*-*gtaB*-Km^R+Δ*acsA*::$P_{cLac143}$-*pmHAS* .

ID	primer name	sequence (5'-3')	ID	primer name	sequence (5'-3')
1001	RP_ acsA _F	ATCCGGCTGTCTAACAAAG	1039	InF_glgA1_F	CCGGGGATCCTCTAG TTTTTCGGCTTCATCGGTC
1002	RP_ acsA _R	GGAATTAATCTCCTACTTGACTTTATG	1040	InF_glgA1_R	GCAGGTCGACTCTAGAGGACATGACGCGAGAATT
1003	InF_pmHAS_to_acsA_F	TAGGAGATTAATTCCATGAATACCCTCAGTCAAGC	1041	RP_glgA1_KO_F	GTTGGGCATAGGTGGGAG
1004	InF_pmHAS_to_acsA_R	GTTAGACAGCCGGATTCTTGTACAGCTCGTTTACA	1042	RP_glgA1_KO_R	ACGCCCAGCTCATTATCCTC
1005	InF_seHasA_to_AcsA_F	ACC CTC AAA AAT CTC ATT ACC GTG	1043	InF_Cm_to_glgA1_F	TAATGAGCTGGGCGT GGCACGTAAGAGGTTCCAAC
1006	InF_seHasA_to_AcsA_R	GTT AGA CAG CCG GAT TCT TGT ACA GCT CGT TTA TTT ATC ATC ATC	1044	InF_Cm_to_ glgA1_R	CCACCTATGCCCAAC GCGTTCTGAACAAATCCAGATG
1007	InF_sfGFP_F	GATGATGATGATAAACGTAAAGGCGAAGAGCTG	1045	ICA_ glmSU_to_glgA1_F	GTGCCGAGGATAATGAGCTGGGCGT TTAACAAAAAAGCAGGAATAAAATTAAC
1008	InF_sfGFP_R	GTTAGACAGCCGGAT TCTAGATTATTATCATCATTTGTACAGTTC	1046	ICA_ glmSU_to_glgA1_R	CAAGTCATAGTCACACATGGTTCTTG TTATTCGACGGTCACACTTT
1009	RP_pmHAS_to_sfGFP_F	ATCCGGCTGTCTAACAAAG	1047	ICA_glgA1_to_glmSU_F	CGCCAAAAGTGTGACCGTCGAATAA CAAGAACCATGTGTGACTATGACTT
1010	RP_pmHAS_to_sfGFP_R	TTTATCATCATCATCCTTGTAATC	1048	ICA_glgA1_to_glmSU_R	AATTTTATTCCTGCTTTTTTGTTAA ACGCCCAGCTCATTATCCTC
1011	RP_seHasA_to_sfGFP_F	ATCCGGCTGTCTAACAAAG	**1049**	**glgA1_seg_F**	**GCGTGACGGCATCAAAAAG**
1012	RP_seHasA_to_sfGFP_R	TTTATCATCATCATCCTTGTAATC	**1050**	**glgA1_seg_R**	**GAGCGCAATACTTGGTGTC**
1013	**acsA_seg_F**	**TTGAAATGGATGAATCGGGTCAACag**	1051	InF_glpK_F	GCAGAATTCGCCCTT TCGCCTTTATGGAGGATGG
1014	**acsA_seg_R**	**GTCCATTACCTCAATGCAGATTACGAAG**	1052	InF_glpK_R	CTGGAATTCGCCCTT GCACTGTGGCAAGGAAATC
1015	IF_tuaD_to_pmHAS_F	GATGATGATAAATAATTAACTTTAAGAAGGAGATATACCATGGG	1053	RP-pCRBlunt-F	AAGGGCGAATTCCAGCAC
1016	IF_tuaD_to_pmHAS_R	GTTAGACAGCCGGATTTAAGCATTATGCGGCCGC	1054	RP-pCRBlunt-R	AAGGGCGAATTCTGCAGAT
1017	RP_143pmHAS_F	ATCCGGCTGTCTAACAAAG	1055	InF_Cm_to_glpK_F	CTATGACTTGCATAGCTGCGTACTCGGTAC
1018	RP_143pmHAS_R	TTATTTATCATCATCATCCTTGTAATCCAAGGTAATGGAATTAATAATAAACTTATTCAC	1056	InF_Cm_to_glpK_R	cgccccgccctgccactc
1019	IF_gtaB_to_pmHAS-tuaD_F	AGATCTCGGGTCCGTGAATCTGTAAgcggccgcataatgcttaa	1057	RP_glpK_F	tggcagggcggggcg TAAAAAAGACTTTATGACTGCTTTACTG
1020	IF_gtaB_to_pmHAS-tuaD_R	GTTAGACAGCCGGAT TTAGATTTCTTCTTTGTTGAGCAAACC	1058	RP_glpK_R	CTATGCAAGTCATAG GGCTCAAAAGACATCATTTAGGG
1021	RP_143pmHAS-tuaD_F	TTTGCTCAACAAAGAAGAAATCTAAatccggctgtctaacaaagc	1059	ICA_ glmSU_to_glpK_F	CTCCCTAAATGATGTCTTTTGAGCC TTAACAAAAAAGCAGGAATAAAATTAAC
1022	RP_143pmHAS-tuaD_R	taagatttaagcattatgcggccgcTTACAGATTCACGGACCCGA	1060	ICA_ glmSU_to_glpK_R	GAGTACGCAGCTATGCAAGTCATAG TTATTCGACGGTCACACTTT
1023	ICA-cpc560_to_DB_F	cttgacgggttttttgtctagatcaACCTGTAGAGAAGAGTCCC	1061	RP_glpK_Cm_F	CGCCAAAAGTGTGACCGTCGAATAA CTATGACTTGCATAGCTGCG
1024	ICA-cpc560_to_DB_R	CCCGATGACGGCAATTTTCTTCATGAATTAATCTCCTACTTGACTTTATGA	1062	RP_glpK_Cm_R	aattttattcctgctttttgttaa GGCTCAAAAGACATCATTTAGGG
1025	RP_143pmDB_F	ATAAAGTCAAGTAGGAGATTAATTCATGAAGAAAATTGCCGTCATC	**1063**	**glpK_seg_F**	**CAACACCATCTATGACTTAGCCCAAATTC**
1026	RP_143pmDB_R	TATTCAGGGACTCTTCTCTACAGGT CCCATGGTATATCTCCTTCTTAA	**1064**	**glpK_seg_R**	**TATCTGTCTGCCATTGCACACC**
1027	InF_glgA2_F	CCGGGGATCCTCTAG ACATCGTCCAGATTGCTTC	1065	ICA_puc19_to_cesA_F	GTATATCGAGCAGCAACAAGACTGAA CATGGTCATAGCTGTTTCCTG
1028	InF_glgA2_R	GCAGGTCGACTCTAG GCAGGGTTCGTAGTTACTG	1066	ICA_puc19_to_cesA_F	CAGCAATACCACCCCGATTGAAGCAC ACTGGCCGTCGTTTTACA
1029	RP_glgA2_KO_F	AAGCCCACTACACCGATATTG	1067	ICA_ cesA _to _puc19 _F	CACGACGTTGTAAAACGACGGCCAGT GTGCTTCAATCGGGGTGGTA
1030	RP_glgA2_KO_R	AAAGTTGTGGATGGTGTAGCAC	1068	ICA_ cesA _to _puc19 _R	CACACAGGAAACAGCTATGACCATG TTCAGTCTTGTTGCTGCTCG
1031	InF_KmR_to_glgA2_F	ACCATCCACAACTTT AATTAATTCTTAGAAAAACTCATCGAGC	1069	RP_cesA_F	TAGGAGACAAGTAAATCATCATTA
1032	InF_KmR_to_glgA2_R	CGGTGTAGTGGGCTT ACAATAAAACTGTCTGCTTACATAAAC	1070	RP_cesA_R	TAAGCTCGCCAAGAAGTTAA
1033	RP_glgA2_to_560DB_F	ACAATTTTGGGACCA AATTAATTCTTAGAAAAACTCATCGAGC	1071	InF_Cm_to_cesA_F	TTCTTGGCGAGCTTA GGCACGTAAGAGGTTCCAAC
1034	RP_glgA2_to_560DB_R	CGGTGTAGTGGGCTT ACAATAAAACTGTCTGCTTACATAAAC	1072	InF_Cm_to_cesA_R	TTTACTTGTCTCCTA GCGTTCTGAACAAATCCAGATG
1035	InF_ 560DB_to_glgA2_F	ACCATCCACAACTTTACCTGTAGAGAAGAGTCCC	**1073**	**cesA_seg_F**	**GGCCATACAAGAGAAATGCG**
1036	InF_ 560DB_to_glgA2_R	TTCTAAGAATTAATTTGGTCCCAAAATTGTCGCC	**1074**	**cesA_seg_R**	**TCATACTTACTTGGTCTGTCAACG**
1037	**glgA2_seg_F**	**TTAGTCTGCGCGGTCATTGT**			
1038	**glgA2_seg_R**	**GTTACTGGGGACGACAAGCA**			

Table S1. List of primers used in this work. Specific primers used for segregation tests were made in black bold.

Strains	Constructs for Syn7002	For Backbone		For Insert	
		Source Plasmid	Primer ID	Source Plasmid or DNA	Primer ID
HA01	pAcsA-cLac143pmHAS	pAcsA-cLac143-YFP	1001, 1002	pUC57-pmHAS	1003, 1004
HA03	pAcsA-cLac143seHasA	pAcsA-cLac143-YFP	1001, 1002	pUC57-seHasA	1005, 1006
HA02	pAcsA-cLac143pmHAS-sfGFP	pAcsA-cLac143pmHAS	1009, 1010	pSR58.6	1007, 1008
HA04	pAcsA-cLac143seHasA-sfGFP	pAcsA-cLac143seHasA	1011, 1012	pSR58.6	1007, 1008
NA	pAcsA-cLac143pmHAS-tuaD	pAcsA-cLac143pmHAS	1017, 1018	pUC57-tuaD	1015, 1016
NA	pAcsA-cLac143pmHAS-tuaD-gtaB	pAcsA-cLac143pmHAS-tuaD	1021, 1022	pUC57-gtaB	1019, 1020
NA	pAcsA-cLac143pmHAS-cpc560-tuaD-gtaB	pAcsA-cLac143pmHAS-tuaD-gtaB	1025, 1026	Syn6803 WT gDNA	1023, 1024
NA	pUC19-glgA2	pUC19	xhoI digested	Syn7002 WT gDNA	1027, 1028
BS06	pUC19-glgA2-Km^R	pUC19-glgA2	1029, 1030	pCRBluntII	1031, 1032
BS13	pUC19-glgA2-cpc560-tuaB-gtaB-Km^R	pUC19-glgA2-Km^R	1033, 1034	pAcsA-cLac143pmHAS-cpc560-tuaD-gtaB	1035, 1036
NA	pUC19-glgA1	pUC19	xhoI digested	Syn7002 WT gDNA	1039, 1040
BS07	pUC19-glgA1-Cm^R	pUC19-glgA1	1041, 1042	pSR58.6	1043, 1044
BS12	pUC19-glgA1-cptSU-Cm^R	pUC19-glgA1-Cm^R	1047, 1048	pUC57-cpt-glmS-glmU	1045, 1046
NA	pCRBlunt-glpK	pCRBluntII	1053, 1054	Syn7002 WT gDNA	1050, 1051
NA	pCRBlunt-glpK-Cm^R	pCRBlunt-glpK	1057, 1058	pSK9	1055, 1056
BS11	pCRBlunt-glpK-cptSU-Cm^R	pCRBlunt-glpK-Cm^R	1061, 1062	pUC57-cpt-glmS-glmU	1059, 1060
NA	pUC19-cesA	pUC19	1065, 1066	Syn7002 WT gDNA	1067, 1068
BS08	pUC19-cesA-Cm^R	pUC19-cesA	1069, 1070	pSR58.6	1071, 1072

Table S2. List of plasmids constructed in this work. Identity of primers used to amplify respective plasmid backbones and inserts are noted in columns “Primer ID”.

Strain	DCW (avg.)	OD_{730}	R-HA	CPS-HA	Intra-HA	Total HA
HA01	0.226±0.009	12.8	0.07%	0.01%	1.4%	1.6%
HA08	0.25±0.014	7.7	1.8%	7.9%	7.1%	16.7%
HA12	0.271±0.011	3.5	6.7%	2.9%	15.3%	24.8%
HA13	0.257±0.018	6.5	1.4%	2.0%	12.9%	16.4%

Table S3. Estimation of total fixed carbon partitioning to HA in different producing strains at day 5 post induction. Total carbon productivity was calculated as previously described (Chwa et al., 2016). Productivities were calculated based on HA quantification shown in Figure 4B, R-HA, CPS-HA and intra-HA amounts, the sum of total HA produced and average dry cell weight (DCW, grams dry cell weight·OD_{730}^{-1}·L^{-1}) measured. HA01: *ΔacsA*::$P_{cLac143}$-*pmHAS*; HA08: Δ*cesA*::Cm^R+Δ*acsA*::$P_{cLac143}$-*pmHAS*; HA12: Δ*glgA1*::P_{cpt}-*glmS-glmU-*Cm^R+Δ*acsA*::$P_{cLac143}$-*pmHAS*; HA13: Δ*glgA2*::P_{cpc560}-*tuaD-gtaB-*Km^R+Δ*acsA*::$P_{cLac143}$-*pmHAS* .